NBS CIRCULAR *557*

Worldwide Radio Noise Levels
Expected in the Frequency Band
10 Kilocycles to 100 Megacycles

UNITED STATES DEPARTMENT OF COMMERCE

NATIONAL BUREAU OF STANDARDS

PERIODICALS OF THE NATIONAL BUREAU OF STANDARDS

(Published monthly)

The National Bureau of Standards is engaged in fundamental and applied research in physics, chemistry, mathematics, and engineering. Projects are conducted in fifteen fields: electricity and electronics, optics and metrology, heat and power, atomic and radiation physics, chemistry, mechanics, organic and fibrous materials, metallurgy, mineral products, building technology, applied mathematics, data processing systems, cryogenic engineering, radio propagation, and radio standards. The Bureau has custody of the national standards of measurement and conducts research leading to the improvement of scientific and engineering standards and of techniques and methods of measurement. Testing methods and instruments are developed; physical constants and properties of materials are determined; and technical processes are investigated.

Journal of Research

The Journal presents research papers by authorities in the specialized fields of physics, mathematics, chemistry, and engineering. Complete details of the work are presented, including laboratory data experimental procedures, and theoretical and mathematical analyses. Annual subscription: domestic, $4.00; $1.25 additional for foreign mailing.

Technical News Bulletin

Summaries of current research at the National Bureau of Standards are published each month in the Technical News Bulletin. The articles are brief, with emphasis on the results of research, chosen on the basis of their scientific or technologic importance. Lists of all Bureau publications during the preceding month are given, including Research Papers, Handbooks, Applied Mathematics Series, Building Materials and Structures Reports, Miscellaneous Publications, and Circulars. Each issue contains 12 or more two-column pages; illustrated. Annual subscription: domestic, $1.00; 35 cents additional for foreign mailing.

Basic Radio Propagation Predictions

The Predictions provide the information necessary for calculating the best frequencies for communication between any two points in the world at any time during the given month. The data are important to all users of long-range radio communications and navigation, including broadcasting, airline, steamship, and wireless services, as well as to investigators of radio propagation and ionosphere. Each issue, covering a period of one month, is released three months in advance and contains 16 large pages, including pertinent charts, drawings, and tables. Annual subscription: domestic, $1.00; 25 cents additional for foreign mailing.

CATALOG OF NBS PUBLICATIONS

National Bureau of Standards Circular 460 and its Supplement list all Bureau publications from 1901 through June 1952, including Applied Mathematics Series, Building Materials and Structures Reports, Circulars, Handbooks, Research Papers, and Miscellaneous Publications. Brief abstracts for the publications issued after January 1, 1942, are also included.

National Bureau of Standards Circular 460, 375 pages, $1.25. Supplement to Circular 460, 223 pages, 75 cents. (A free mimeographed list of publications issued since June 1952 is available on request to the National Bureau of Standards.)

Worldwide Radio Noise Levels Expected in the Frequency Band 10 Kilocycles to 100 Megacycles

W. Q. Crichlow, D. F. Smith
R. N. Morton, and W. R. Corliss

Contents

II

WORLDWIDE RADIO NOISE LEVELS EXPECTED IN THE FREQUENCY BAND 10 KILOCYCLES TO 100 MEGACYCLES

W. Q. Crichlow, D. F. Smith, R. N. Morton, and W. R. Corliss

External radio noise levels are presented in the form of an effective antenna noise figure F_a, which is defined as the noise power available from an equivalent lossless antenna relative to kt_0b (the thermal noise power available from the passive resistance of a circuit with bandwidth, b, and at the standard absolute temperature, t_0). This form of expressing the noise has been chosen for convenience in combining for practical applications the noise received external to the antenna with the noise already present in the receiver. This form of presentation includes the frequency squared factor arising from the absorbing area of the receiving antenna and provides a measure of noise directly applicable to the "transmission-loss" method of measuring radio propagation.

Curves are given that show the expected median levels of radio noise during 4-hour time blocks for each season. The curves also show the effects of frequency and geographical location (using noise grade maps) and include atmospheric, galactic, and manmade noise sources.

The expected median values of atmospheric noise levels were largely based on the information given in the National Bureau of Standards Circular 462.

Also, the expected variability of noise levels within the 4-hour time blocks is given in terms of the ratios of the upper decile to medain level and median to lower decile level. These ratios are shown to be a function of frequency, time of day, and median noise-level amplitude.

The results of measurements at Boulder, Colo., Front Royal, Va., and Tatsfield, England, are shown in comparison with the expected levels.

1. Introduction

The determination of the minimum signal level required for satisfactory radio reception in the absence of other undesired radio signals necessitates a knowledge of the noise with which the desired signal must compete at the receiving location. This noise may originate within the receiving system or arise from sources external to the antenna. At frequencies less than about 15 Mc, thunderstorms usually represent the principal source of the external noise, although the contribution from manmade sources is sometimes dominant, particularly during those times when the noise from thunderstorms is low. In the frequency range 15 to 150 Mc, the external noise is principally from cosmic sources, i. e., of galactic and solar origin, although in this range manmade noise will also predominate at times in some locations. When the ionospheric critical frequency is low, as is the case particularly in the Arctic regions, galactic noise might be the principal source of external noise even at frequencies of 1 Mc or lower.

Studies of radio-noise levels have been in progress at the National Bureau of Standards and elsewhere [1] [1] for a number of years, and predictions of worldwide noise levels have been published [2, 3, 4]. The initial research leading to these publications was carried out in 1942 by a group in England at the Interservices Ionosphere Bureau (primarily by D. K. Bailey and J. S. Kojan, at that time officers in the United States Signal Corps) and in the United States at the Interservice Radio Propagation Laboratory (primarily by Newbern Smith).

It is the purpose of this report to present new predictions that are based on these earlier publications but which contain additional information and are in a more useful basic form. More results of noise measurements are gradually becoming available, and a further revision of the predictions is in preparation. It is intended, however, that in later revisions the basic method of describing the noise level will be that used in this report.

2. Terms of Reference

The ultimate use of a prediction of radio-noise level is to compare it with a signal level in such a way that the resulting signal-to-noise ratio can be determined, and thus a grade of service may be established for a given set of terminal facilities and propagation path, or the required terminal facilities can be determined to provide a given grade of service.

As the noise level may result from a combination of external noise as well as noise generated within the receiver, it is convenient to express the resulting noise by means of a generalization of Friis' [5] definition of the noise figure of a radio receiver, which has recently been applied to the solution of radio-propagation problems by Norton [6].

Figure 1 is a block diagram in which the various elements that contribute to the resultant noise level are shown. Network (a) is taken as a loss-free antenna with an average available noise power, p_n, which results exclusively from external noise sources. The noise figure, f_a, of network (a) can then be defined by

$$f_a \equiv \frac{p_n}{kt_0b},\qquad(1)$$

[1] Figures in brackets indicate the literature references at the end of this paper.

1

where

$k=$ Boltzmann's constant $=1.3802\times10^{-23}$ j/°K
$t_0=$ reference room temperature in degrees Kelvin at which the noise-figure measurements are to be made or to which they are to be adjusted
$b=$ effective noise bandwidth in cycles per second.

Most of the remainder of this paper deals with predictions and measured values of f_a.

The losses [2], l_c, in the antenna and associated circuit are represented in network (c), whose noise figure, f_c, is

$$f_c = l_c \frac{t_c}{t_0}, \qquad (2)$$

where t_c is the actual temperature in degrees Kelvin of the antenna and nearby ground. Similarly, the transmission-line loss (see footnote 2) l_t, and temperature t_t, will determine a noise figure, f_t, for the transmission line, which is given by

$$f_t = l_t \frac{t_t}{t_0}. \qquad (2a)$$

The receiver noise figure is designated by f_r. Using Friis' method of combining the noise figures of several networks in cascade, the effective noise figure at the input of the antenna is given by

$$f \equiv f_{actr} = f_a - 1 + l_c\left(\frac{t_c}{t_0}-1\right) + l_c l_t\left(\frac{t_t}{t_0}-1\right) + l_c l_t f_r. \quad (2b)$$

If we take the temperature of all networks equal to t_0, (2b) becomes

$$f = f_a - 1 + f_c f_t f_r. \qquad (2c)$$

Taking r as the minimum signal-to-noise power ratio that will provide satisfactory service, the minimum signal power, in watts, available at the input of the antenna that will provide satisfactory reception may be expressed

$$p_m = r f k t_0 b. \qquad (3)$$

Expressed in decibels above 1 w, (3) becomes [3]

$$P_m = R + F + B - 204.00, \qquad (4)$$

where $R = 10 \log_{10} r$, $F = 10 \log_{10} f$, $B = 10 \log_{10} b$.

In the above it was found convenient to set $10 \log_{10} kt_0 \equiv 204.00$; a recent determination [7] of Boltzmann's constant $k = 1.3802 \times 10^{-23} j$/°K, so that our convention is satisfied if the reference

temperature t_0 for the determination of effective noise figure is taken to be 288.44 °K.

In evaluating the effective receiver noise figure, F, for use in (4), it is necessary to consider the magnitudes of each of the parameters, f_a, f_c, f_t, and f_r. In many cases, where a reasonably efficient antenna system is used in conjunction with a moderately low noise-figure receiver, f_a will predominate, and F will be equal to F_a. This relationship holds at low frequencies because of the extremely high values of F_a that exist and even with a relatively poor receiving system, F_a will still tend to predominate most of the time. At the higher frequencies the values of F_a are lower, but as the antenna system tends to become more efficient, particularly when horizontal antennas are used, antenna losses can frequently be neglected, and f_c approaches unity. Thus at these higher frequencies it is necessary in general to consider only the effect of f_a, f_t, and f_r when evaluating f. Values of f_t and f_r may be obtained by direct measurement of the transmission-line loss and the receiver noise figure. However, in those cases where the antenna losses are important, such as at the lower frequencies with short vertical antennas near the ground, the value of f_c must be obtained by indirect means. Frequently an estimate of these losses can be made by impedance measurements in conjunction with a calculation of the radiation resistance.

As an example of a method of determining f_c at these lower frequencies, a discussion is presented below for the case of a short vertical antenna. The equivalent circuit for such an antenna is shown in figure 2, where e_a is the voltage induced in the antenna, x_a the antenna capacitive reactance, r_a the radiation resistance, r_g the ground loss resistance, r_i the insulator and circuit loss resistance, and x_i the insulator and circuit capacitive reactance. For high-Q antennas with low-loss insulators, which is usually the case when using a vertical antenna whose height is less than an eighth wavelength, the antenna loss can be expressed by

$$f_c = \frac{p_n}{p_a} = \frac{r_m x_i^2}{r_a(x_i - x_m)^2}, \qquad (5)$$

where

$p_a=$ available power from the actual antenna
$r_m = \dfrac{x_i^2[r_i(r_a+r_g)+x_a^2]}{r_i(x_a+x_i)^2} =$ resistive component of measured antenna impedance, z_m
$x_m = \dfrac{x_a x_i}{x_a+x_i} =$ reactive component of measured impedance, z_m.

The radiation resistance, r_a, in ohms for a short cylindrical antenna perpendicular to a perfectly conducting plane is given by [8]

$$r_a = 40\pi^2 \frac{h^2}{\lambda^2}, \qquad (6)$$

[2] Loss is taken here as the ratio of available input power to available output power. It will differ from the loss in delivered power, unless a matched load is used.
[3] Throughout this paper capital letters will be used to denote the ratios expressed in decibels, of corresponding quantities designated with lowercase type.

where

h = length of the antenna in meters

λ = wavelength in meters.

When the insulator and circuit losses are negligible, eq (5) simplifies to

$$f_c = \frac{r_a + r_g}{r_a}, \quad (r_i \gg r_m). \tag{6a}$$

The quantities r_m, x_m, and x_i can be either measured at the antenna terminals or computed from the basic antenna-circuit elements. The most accurate and direct method is by measurement. The value of f_c can be obtained by similar methods for other types of antennas.

3. Characteristics of Radio Noise

This paper deals with external radio noise of three types; namely, atmospheric, galactic, and manmade. Each type has different characteristics and thus will be discussed separately.

Of the three types, atmospheric noise is the most erratic in character, consisting in general of short pulses with random recurrence—superimposed upon a background of random noise. If these short time variations of instantaneous noise power are averaged over a period of several minutes, this average power level is found to be relatively constant during a given hour, the variations seldom exceeding 2 or 3 db, except during sunrise or sunset periods. The median value of this average noise power within the hour has been taken as the basic unit in this paper and will be referred to as its hourly median or hourly value.

The hourly values of the noise vary with time of day because of changing propagation conditions and frequency of thunderstorms, but fortunately this variation tends to follow a particular pattern. At the lower frequencies, the nighttime noise is high because noise is propagated by means of the ionosphere from storms at large distances. During the daytime, the ionospheric absorption is high, and the noise received from distant storms is reduced, the received noise being principally from local storms. Local storms tend to predominate during the afternoon hours, and therefore the noise level is enhanced somewhat during those hours. Thus we have maximum noise levels at night, minimum during the morning, a moderate increase in the afternoon, and again high levels at night.

At the higher frequencies, the shape of the diurnal curve tends to reverse itself because the ionosphere will support propagation only during the daylight hours. Actually, at these frequencies the diurnal curve of the received noise becomes relatively flat because of the presence of galactic and manmade noise.

There is also a regular seasonal trend to the noise that is influenced by ionospheric absorption, as well as the location and number of thunderstorms. The thunderstorm centers tend to shift above and below the equator from summer to winter, and in addition the ionospheric absorption is higher in the summer, which tends to offset the increased thunderstorm activity at that time. Nevertheless, the received noise tends to be highest in the summer and lowest in the winter at tropical and temperate latitudes.

The received noise level varies with frequency because the noise radiated by the thunderstorm and its efficiency of propagation are functions of frequency. In general, the received noise level decreases with increasing frequency.

There are variations in the noise level with geographic location, the highest levels being encountered in equatorial regions and the lowest levels in the polar regions. The received noise levels are influenced by topography, as well as weather and propagation conditions.

There are also variations in received noise levels with sunspot activity, but no attempt has been made to take this into account in this paper.

In the prediction curves that follow, those variables for which the noise has definite trends, i. e., time of day, season, frequency, and geographic location, have been taken into account directly. However, there are certain unpredictable variations which can be taken into account statistically. For example, at a particular time of day and season, the hourly value will vary from day to day because of random changes in thunderstorm activity and propagation conditions. Because of this random variability, it has been found desirable to designate time blocks for prediction purposes. Each time block is for four consecutive hours within a given season. The median of the hourly values within the time block is referred to as the time-block median. Deviations of the hourly values from the time-block median are expressed in terms of the upper and lower decile values of the cumulative distribution of the hourly values.

The limits of the time blocks were chosen as 0000 to 0400, 0400 to 0800, 0800 to 1200, etc., so that the sunrise-sunset periods changing through the seasons would fall within only the 0400 to 0800 and 1600 to 2000 time blocks. Also this choice of time-block limits prevents splitting a time block between successive days.

Figure 3 is an example of the distribution of the hourly values within a time block. The ordinate is in decibels, and the abscissa is a cumulative normal probability scale. The curve shows the percentage of the hours during the time block that various levels are exceeded. It may be noted that the curve can be represented with reasonable accuracy by two straight lines,[4] one of which passes through the upper decile and median, and another through the median and lower decile. In this paper the median value for the time block is designated by the symbol, F_{am}, and the ratios of the upper decile to median and of the median to the lower decile are designated by the symbols D_u and D_l, respectively, as illus-

---

[4] This approach is justified by its repeated successful application to a large number of curves of this type.

trated on figure 3. Thus, a knowledge of these three values, which can be obtained from the predictions in this paper, will enable an estimate to be made of any percentile value for the time block.

Manmade noise may arise from any number of sources, such as power lines, industrial machinery, diathermy machines, ignition systems, etc., and thus its characteristics vary over wide limits. It is propagated to the receiver principally by conduction over power lines or by ground-wave propagation from the source and is thus relatively unaffected by diurnal or seasonal changes in the ionosphere. There is no definite geographic effect except for the proximity of the receiving location to a metropolitan area, and studies to date of its variation with location are inadequate for evaluation. In this paper the only trend in manmade noise that has been considered is the variation with frequency. The level of this noise decreases with increasing frequency, owing in part to the radiated spectrum and partly because of propagation.

Galactic noise has the same character as thermal noise and thus has a Gaussian amplitude-time distribution as received from any one portion of the sky. Its average intensity is approximately proportional to the minus 2.3 power of the frequency. The maximum intensity of galactic noise is from the direction of the constellation Sagittarius, and thus as this constellation passes across the pattern of the receiving antenna, the average received power changes. If it were not for the presence of the ionosphere, the variations in galactic noise for a particular receiving antenna and location would repeat themselves each sidereal day, and precise predictions could be made for any time in the future. However, because of the screening effect of the ionosphere at low frequencies, the galactic noise level that is actually received depends upon the absorption characteristics of the ionosphere and the relationship of the operating frequency to the vertical incidence critical frequency. In most cases the F-layer is responsible for these effects.

In Arctic regions, where very low critical frequencies are often encountered galactic noise may accordingly be expected to represent the principal source of external noise even at 1 Mc and lower. Unpublished measurements furnished to the authors by Ross Bateman and Richard C. Kirby indicated that the principal noise was of galactic origin at 8 Mc during most of a 3-day period at Point Barrow, Alaska. The noise fluctuations appeared to have the same character as those of thermal noise, and the level was in agreement with the frequency law for galactic noise when compared with simultaneous measurements at 24 and 48 Mc.

At temperate and tropical latitudes, where atmospherics are stronger and critical frequencies are lower, galactic noise is usually negligible below about 15 Mc, and above this frequency it can be predicted accurately. This transition frequency is not fixed but will vary with geographical location and phase of the sunspot cycle.

In this paper, galactic noise has also been evaluated by time blocks, and as there are changes in intensity with time and season, predictions are given as with the other types of noise for the median, upper decile, and lower decile values for the same time blocks.

4. Discussion of Noise Predictions

Figures 4 to 7 [5] are maps which show the distribution of noise grades throughout the world for each season of the year. Areas in which thunderstorms are most frequent are indicated by the higher noise grades and are generally found in equatorial regions. The areas most remote from the principal thunderstorm areas and in which low atmospheric noise levels may be expected, even by way of long distance sky-wave propagation, are indicated by the lower noise grades.

Values of the expected atmospheric noise levels, corresponding to the noise grades on the world maps, are shown in figures 8 to 31. The levels are given in terms of the time-block median antenna noise figure, F_{am}, which was defined above, and these levels represent the median noise expected from a short vertical antenna. They are, thus, strictly applicable only when applied to reception with a short vertical antenna. However these curves can be used for approximately predicting the external noise expected on other types of antennas, provided the effects of polarization and directivity on the noise are either negligible or are taken into account. The received noise will also be influenced by ground conductivity, but because of the many possible propagation paths, no attempt has been made to take this into account. Each curve is for the median value of the average noise power during the stated 4-hour time block and season of the year, and is plotted as a function of frequency.

Values of galactic noise are also shown on these figures. The values given represent the time-block medians to be expected when the ionosphere will allow penetration, i. e., at frequencies above the critical frequency. The degree of penetration at frequencies below about 15 Mc will vary with time and location, and when the predicted atmospherics are less than the predicted galactic noise, the limiting noise may fall anywhere between the two curves, depending upon ionospheric conditions. Above about 15 Mc, the variations of galactic noise are small and are shown in appendix 4 to be less than ±2 db at any latitude or time.

In addition to values of atmospheric and galactic noise, a curve is also shown on these figures, which gives the expected values of radio noise due to manmade sources. This curve was obtained from measurements during daylight hours when atmospherics were not audible, and is representative of a nonmetropolitan recording site that has been chosen with reasonable care to avoid man-made noise.

---

[5] These figures were taken directly from reference 2 without change.

Figures 32 and 33 show the day-to-day variation to be expected about the median noise level during the 4-hour time blocks for all sources of noise. The variations are expressed in terms of the ratio of the upper decile to the median and the ratio of the median to the lower decile value, both ratios expressed in decibels.

Figure 32 shows these ratios of upper decile to median and median to lower decile to be expected within the time blocks as a function of the median level of the time block without regard to frequency, time, or season. Although there is a definite relationship between these ratios and the time-block medians, it is more convenient for prediction purposes to determine them as a function of frequency and time, as shown on figure 33. Thus if it is desired to determine the noise level that is exceeded for 10 percent of the hours within a time block, the value of the upper decile ratio, D_u, from figure 33 is chosen for the desired operating frequency and time block and added to the corresponding median value of F_{am} obtained from the prediction curves of figures 8 to 31.

5. Comparison with Measurements

For comparison purposes, the results of recent measurements have also been plotted on figures 8 to 31. A year's data are represented by the plotted points from observations at Front Royal, Va., Boulder, Colo, and Tatsfield, England. The noise grades for these three stations range from 2 to 3 for all seasons, and thus the points would be expected to lie between the curves for these two noise grades, except where manmade and galactic noise levels exceed the atmospherics. Inspection of the figures will show that there is considerable scatter of the points, and in some isolated cases the observed medians are outside of the limits of noise grades 1 to 5. The deviations from the predictions do not appear to be systematic, however, and no satisfactory way of further modifying the predictions is apparent at this time.

In order to make an estimate of the errors involved in using the prediction curves, the deviations of the measured time-block medians from their corresponding predicted values were studied. As the predictions are for three sources of noise, i. e., atmospheric, manmade, and galactic, the highest of the three [6] was taken as being the controlling source. The study showed that the average of all deviations was 1.7 db above the prediction and that the root-mean-square deviation was 8.9 db. Cumulative distributions of these deviations have been plotted in figure 34 by stations. It may be seen that the medians of the distributions for Front Royal and Tatsfield are very close to zero decibels, whereas the median of the Boulder distribution is +9 db. This indicates that on the average, noise levels predicted for Front Royal and Tatsfield would be very nearly correct, whereas levels predicted

[6] This process will introduce no more than a 3-db error when only two sources of interference are present.

for Boulder would generally be too low. Therefore, it may be concluded that the maps in figures 4 to 7 indicate too low a noise grade for the Boulder area, but are about right for Front Royal and Tatsfield. The combined distribution of the measured time-block medians for all three stations is also shown in figure 34 and can be used in estimating the errors to be expected in making a prediction of the noise level at any location in general. For example, if it is desired to protect a radio service against the noise with probability of 0.9 that the service will be satisfactory, then the 10-percent value, 14 db, from the combined distribution should be added as a safety factor to the value of F_{am} obtained from the prediction curves.

Actually, it is believed that the errors will be somewhat less than indicated by these distributions because some of the higher observed values are known to contain signal contamination and are thus not representative of the true noise level. Also, there are equipment instabilities that cause errors in the observations. With improved equipment currently being manufactured for the Central Radio Propagation Laboratory of the National Bureau of Standards, it is believed that the above sources of error will be largely eliminated. With the more accurate data thus available, it is expected that revised predictions will be available in the very near future. These revisions will take the form of changes in the level of the curves on figures 8 to 31 as well as a modification of the location of the contours on the maps in figures 4 to 7.

The results of the measurements are also shown in diurnal plots of the time-block median values of F_{am} in figures 35 to 37. The solid lines represent the observed median values, and these are plotted for comparison with the appropriate predicted value of atmospheric, manmade, or galactic noise.

The variations of the measured hourly values about the medians of the time blocks are shown in figures 38 to 40. The solid lines represent the ratio, D_u, of the upper decile value to the median, and the dashed lines represent the ratio, D_l, of the median to the lower decile value, both ratios expressed in decibels. These figures show in general that the variations are greatest during the sunrise and sunset periods when the propagation is changing from day to night conditions. The variations shown on these figures were used to obtain the smoothed variation curves in figures 32 and 33.

Measurements of galactic noise were made at Boulder, Colo. on 20 Mc by operating the receiver on short time constant and scaling the bottom of the trace, thus eliminating the effects of atmospherics and manmade noise. These measurements, in conjunction with an integration of Reber's [9, 10, 11, 12] contours, were used to calculate the expected values of galactic noise as received on a half-wave vertical antenna at any

latitude (see appendix 4). The results of this study are given in figure 41, which shows galactic noise as a function of sidereal time for various latitudes.

As galactic noise is a function of sidereal time, a galactic-noise maximum will occur about 4 minutes earlier each day, thus causing variations in the time blocks that progress seasonally. The median values of the resulting galactic-noise variation for each time block are shown in figure 42. These galactic-noise values were determined for 20 Mc but are applicable to any frequency, f_{Mc}, by subtracting $23 \log_{10}(f_{Mc}/20)$. The variations of the hourly values within the time blocks are shown on figure 43 in terms of the upper decile to median and median to lower decile ratios, D_u and D_l, and are applicable on any frequency between 10 and 100 Mc.

6. Application to System Problems

The minimum receiving antenna signal power required for satisfactory service is discussed in section 2 and can be obtained from eq (4). In order to determine the power that must be radiated from the transmitting antenna to produce the required signal power at the receiving antenna, it is convenient to make use of the concept of "transmission loss", which has been defined by Norton [6] as

$$\text{Transmission loss} \equiv L \equiv 10 \log_{10} \left[\frac{\text{Power radiated from the transmitting antenna}}{\text{Resulting signal power available from the loss-free receiving antenna}} \right] \quad (7)$$

Thus, expressed in decibels above 1 w, the required radiated power is

$$P_r = L + P_m. \quad (8)$$

Transmission loss, L, as defined above, excludes transmitting- and receiving-antenna circuit losses, as well as losses in transmission lines at the transmitter or receiver. It is a measure of the loss that is attributable solely to the transmission medium, including the effective gains of the transmitting and receiving antennas.

It is sometimes possible to separate L into its component parts as given by

$$L = L_b - G_p + A, \quad (9)$$

where

$L_b = 20 \log_{10} (4\pi d/\lambda) =$ transmission loss for isotropic transmitting and receiving antennas separated a distance, d, in free space

$G_p =$ the "path antenna gain"
$A =$ the propagation path attenuation relative to the free-space value.

Expressing the distance, d, in miles and the frequency, f_{Mc}, in megacycles, the basic transmission loss in free space can be expressed as

$$L_b = 20 \log_{10} d + 20 \log_{10} f_{Mc} + 36.581. \quad (10)$$

The "path antenna gain" is the combined "effective" gain of the transmitting and receiving antennas relative to that of isotropic antennas. Note that this effective antenna gain for the path is generally somewhat less than the sum of the transmitting and receiving antenna gains with optimum orientation in free space. If G_t and G_r are taken as the transmitting and receiving antenna gains in the direction of the predominant mode of propagation, G_p is approximately equal to $G_t + G_r$.

Combining (4) and (8) and letting L_t, expressed in decibels, denote the transmitting-antenna circuit losses, together with the transmitting-antenna transmission-line losses; the required transmitter power, P_t, in decibels above 1 w is

$$P_t = L_t + L + R + F + B - 204. \quad (11)$$

The required signal-to-noise ratio, R, is generally established for a given percentage of intelligibility, percentage of accuracy, or degree of freedom from annoyance. Its value will depend upon the type of service (broadcasting, telephone communication, aural telegraph, automatic telegraph, etc.), and in many cases upon the character of the noise. For example, the characteristics of thermal noise can be described by a Gaussian amplitude-time distribution, and whenever this type of noise limits reception, the value of R, once established, will always provide the same grade of service. On the other hand, atmospheric radio noise has extremely variable characteristics that cannot be described mathematically. For those types of service that are affected by the character of the noise, as well as its average level, R may depend upon time, frequency, and geographic location.

R is usually determined under steady state conditions, i. e., when the average signal and noise levels are constant and under conditions where the characteristics of the noise are either known or of a constant nature. The results, therefore, are applicable to situations in which propagation of the signal is by means of its ground wave and during periods of time within which the noise level and characteristics are essentially constant.

When propagation of the signal is by means of the ionosphere or troposphere and the noise is of atmospheric origin, a value of R determined under steady state conditions is no longer applicable because the signal power will vary with time (i. e., fade) owing in part to phase interference between components arriving along the various transmission paths, which results in a

6

Rayleigh distribution [13] of the received signal. These signal variations in conjunction with the erratic characteristics of the atmospherics necessitate a determination of a different signal-to-noise ratio to provide a particular grade of service. Under these conditions it is customary to express the received signal and noise powers in terms of their hourly median values. An experimental determination must then be made of the median-signal-to-median-noise ratio, R_h, required to provide the desired grade of service during the hour. The value of R_h, thus determined, is applicable only for the same type of fading and the same type of noise.

Once R_h has been determined, and letting L_h represent the median transmission loss for the hour, the required transmitter power is given by

$$P_t = L_t + L_h + R_h + F + B - 204. \qquad (12)$$

It has been shown experimentally that the hourly median ionospheric or tropospheric fields, P_h, for a given hour of the day and a given month of the year are log-normally distributed [14, 15]. It follows directly then that the hourly median transmission loss, L_h, expressed in decibels, is normally distributed; thus a complete description of the expected distribution of the hourly median transmission loss for any given time of day and season can be expressed in terms of two parameters, the time-block median, L_m, and the upper decile value, L_d. The quantity $(L_d - L_m)$ is a measure of the variability of the hourly median transmission loss and is designated by D_s. Thus L_m and D_s completely describe the distribution of L_h.

For a given time of day and season of the year, the hourly values of received noise, F_a, are also variable from day to day. The median value for each season and time of day has been designated as the time-block median, F_{am}, and is given in figures 8 to 31. As values of F_{am} are given for three sources of noise, i. e., atmospheric, manmade, and galactic, the highest of the three should be taken as the controlling source. Ratios of the upper decile to median, D_u, and median to lower decile, D_l, expressed in decibels, are given in figure 33.

The received noise can be represented with reasonable accuracy by assuming a normal distribution of F_a with a median value of F_{am} and upper decile ratio, D_u.

Now, if it is desired to provide a grade of service represented by the hourly median signal-to-noise ratio, R_h, for x percent of the hours within a time block, then a protection factor, T_x, must be provided so that R_h will be exceeded for the required percentage of time. As the values of L_h are normally distributed and the values of F_a can be considered to approximate a normal distribution, the protection factor, T_x, in decibels necessary to provide service for x percent of the time block is given by

$$T_x = f(x) \sqrt{D_s^2 + D_u^2 + 2cD_sD_u}, \qquad (13)$$

where c is the correlation coefficient between L_h and F_a.

Values of $f(x)$ are given in table 1. They were calculated from a normal distribution having a mean value of zero and an upper decile value of unity. $f(x)$ is equal to the value of this distribution exceeded for $(100-x)$ percent of the time.

TABLE 1. *Values of f (x) versus x*

Percentage of time, x	$f(x)$
99.99	2.902
99.9	2.411
99	1.815
95	1.284
90	1.000
80	0.657
70	0.409
60	0.198
50	0.000
40	−0.198
30	−0.409
20	−0.657
10	−1.000
5	−1.284
1	−1.815
0.1	−2.411
0.01	−2.902

As the cumulative amplitude-time distribution of F_a is somewhat skewed (i. e., D_u is not exactly equal to D_l), eq (13) will only approximate the true protection factor. However, a graphical solution, using the actual distributions encountered in practice, indicated that the errors would be small. When the percentage of time to be protected is less than 50 percent, better accuracy will be obtained by substituting D_l for D_u in eq (13).

For those cases where the effective noise figure, F, is determined by the received noise, F_a, the transmitter power that is required to give satisfactory service during x percent of the hours of a time block is given by

$$P_t = L_t + L_m + T_x + R_h + F_{am} + B - 204. \qquad (14)$$

Predictions of values of L_m can be made with reasonable accuracy. However, a degree of uncertainty still remains in the prediction of values of F_{am}. Use of (14) will result in a probability of 0.5 that at least the desired grade of service will be achieved. This means that since the value of F_{am} is not known exactly, that one-half of the circuits established by (14) will be likely to give better than the specified grade of service and that one-half of them will probably give worse. In order to increase the probability of producing the desired grade of service, it is sometimes desirable to use a larger value of P_t than calculated above. Figure 34 can be used in estimating the necessary increase in P_t to give a certain probability of service. For example, if the calculated value of P_t is increased by 14 db, which corresponds to the value by which F_{am} exceeded the prediction in 10 percent of the observations, then the probability of achieving the desired grade of service for x percent of the time is $1 - 0.1 = 0.9$.

For those cases in which the limiting noise is internal rather than external to the antenna

$(F \gg F_{am})$, P_t can be calculated from (13) and (14) by letting $D_u = 0$ and replacing F_{am} by F.

In order to illustrate the application of the above principles, the following examples will be evaluated:

EXAMPLE 1: Steady Signal and Steady Noise. Determine the required transmitter power for standard broadcast service under the following conditions:

Transmitting antenna	Half-wave vertical.
Receiving antenna	10-ft vertical whip.
Frequency	1,450 kc.
Ground conductivity	10^{-13} emu.
Time	August daytime.
Distance	20 miles.
Receiver	High quality.
Noise grade	3-summer.

The required transmitter power can be obtained by evaluating eq (11) as follows:

1. With reasonable care the transmitter transmission-line loss can be made negligible and thus L_t is taken as 0 db.

2. The transmission loss, L, is evaluated from eq (9). From eq (10), the basic transmission loss, L_b, is $L_b = 26.02 + 3.23 + 36.58 = 65.85$ db. The transmitting-antenna gain, G_t, for a half-wave grounded antenna is equal to 6.84 db. The receiving-antenna gain, G_r, for a short vertical monopole, receiving a ground wave is -1.25 db.

The attenuation, A, relative to the free-space value can be determined from the ground-wave field-strength curve [16] for a frequency of 1,450 kc and a conductivity of 10^{-13} emu. It is numerically equal to the decibel difference between the inverse distance field strength and the 10^{-13} emu field-strength curve. At 20 miles, A is equal to 14 db.

Rounding off all quantities to the nearest decibel L is given by $L = 66 - 7 + 1 + 14 = 74$ db.

3. The required signal-to-noise ratio, R, has been established by the CCIR [17]. For broadcasting, the *peak* signal-to-rms noise in a 6-kc bandwidth is given as 47 db. Subtracting 6 db, we obtain the required *carrier*-to-rms noise, and subtracting 2 db to correct to a 10-kc band, $R = 39$ db.

4. The effective receiver noise figure, F, is given by eq (2). The antenna noise figure, F_a, is determined by manmade noise, and from figures 22 and 23 is equal to 50 db ($f_a = 10^5$).

Taking an antenna ground-loss resistance of 5 ohms, a radiation resistance of 0.086 ohms, and neglecting insulator loss, the antenna loss factor, f_c (eq 6 and 6a), is equal to $(5 + 0.086)/0.086 = 59$. The transmission-line loss factor, f_t, can be considered equal to unity for the present example.

The noise figure, f_r, of a typical high quality receiver measured from a matched source will be approximately 10^2; however, with such a short receiving antenna it will be much higher because of the mismatch. For the present example, a value of 2×10^5 will be assumed.

Thus f is $f = 10^5 - 1 + 59 \times 2 \times 10^5 = 1.18 \times 10^7$, or $F = 71$ db.

It may be noted that in this example the value of f is determined by $f_c f_t f_r$, and thus reception is limited by set noise rather than received noise. (With a better antenna and a lower noise-figure receiver, received noise could be made the controlling factor and the required transmitter power would be less.)

5. The bandwidth has been taken as 10 kc, and thus $B = 40$ db. Therefore, the required transmitter power is $P_t = 0 + 74 + 39 + 71 + 40 - 204 = 20$ db, or 100 w.

EXAMPLE 2: Variable Signal and Variable Noise. Determine the required transmitter power for an A-3 voice communication service under the following conditions:

Transmitting antenna	Half wave vertical.
Receiving antenna	30-ft vertical whip.
Frequency	2 Mc.
Time	8 p. m. to 12 p. m., August.
Distance	500 miles.
Receiver	Communications type.
Noise grade	3.
Intelligibility	90 percent.
Grade of service	90 percent of time.

The required transmitter power can be obtained by evaluating (14) as follows:

1. As in example 1, L_t can be assumed equal to 0.

2. The time-block median value of the transmission loss, L_m, can be evaluated from eq (9) by replacing L with L_m and A with A_m, where A_m is the time-block median value of A.

Assuming single hop E-layer propagation with a virtual height of 105 km, the actual triangular path length for a 500-mile great circle distance is 520 miles. Thus the basic transmission loss, L_b, is $L_b = 54.32 + 6.02 + 36.58 = 96.92$ db.

The angle of radiation for this path can be determined from [18], page 11, and is 13°.

This value of P_t will provide the required grade of service, with a probability of about 0.5. As an added safety factor it is sometimes desirable to increase the transmitter power so that the probability of service will be greater. From figure 34 it can be seen that adding 14 db will give a probability of service of about 0.9 because of uncertainties in determining the correct value of F_{am}. This would result in a required transmitter power of 7.9 kw.

It should be noted that in the above examples, assumptions have been made of the magnitude of a number of the parameters used in the calculations. In an actual situation these parameters should be determined as accurately as possible before an evaluation of the over-all system performance is attempted.

From page 61 of [18], assuming "good" ground, the transmitting-antenna gain relative to a short vertical monopole, at an angle of 13° is $530/1000 = 0.53$. The gain, G_t relative to an isotropic antenna is $0.53 \times 3 = 1.59$, or 2 db.

From pages 15 and 55 of [18], the receiving-antenna gain relative to a short vertical monopole is $43/93 = 0.46$. Thus $G_r = 0.46 \times 3 = 1.38$, or 1.4 db.

The time-block median value of the attenuation relative to free space, A_m, is determined as follows: For this time and frequency, the ionospheric absorption is taken as zero. The polarization loss is taken as 3 db, and a loss of 1.6 db is taken, since the median of a Rayleigh distribution is 1.6 db less than its rms value. Therefore, the value of A_m is $3+1.6=4.6$ db.

Rounding off to the nearest decibel, the resulting value of L_m is $L_m=97-2-1+5=99$ db.

3. The long time variations of signal and noise within the time block are taken into account by means of eq(13). For a protection of service for 90 percent of the time, $f(x)=1$. The upper decile value of the signal, D_s, from [14], is 6 db, and from figure 33, the upper decile value of the noise, D_u, is 8.75 db. Assuming a correlation coefficient of zero between the signal and noise, the protection factor $T_x=11$ db.

4. The required peak signal-to-rms noise ratio for low-grade telephony is obtained from [17] as 15 db. The carrier-to-noise ratio is, therefore 9 db. Adding 8 db to provide service 90 percent of the hour in the presence of Rayleigh fading, the value of R_h is 17 db.

5. The value of F_{am} from figure 25 is 64 db. With a 30-ft receiving antenna and a good communications receiver, $10 \log f_c f_t f_r$ is much less than 64 db, and thus the reception is limited by the external noise, F_{am}.

6. The receiver bandwidth is taken as 6 kc and $B=39$ db. Therefore, the required transmitter power is $P_t=0+99+11+17+64+38-204=25$ db, or 315 w.

7. Appendix 1. Measurement Techniques

Measurements of radio noise levels are being made by the Central Radio Propagation Laboratory of the National Bureau of Standards at two field stations, one at Front Royal, Va., and the other at Boulder, Colo. For use at these stations, a standard antenna system was developed, which consists of a 21.75-ft vertical whip in the center of an elevated ground plane. The ground plane, which stabilizes the impedance of the antenna and improves its efficiency, contains 90 radials 100 feet long, and is 8 feet above the ground.

The recording equipment is sheltered by a small house under the radial system, the roof of which supports the antenna with a low-loss, low-capacitance insulator. A special network has been designed that couples the antenna efficiently at six frequencies to individual preamplifiers. Separate receivers are used at each frequency, and include commercial receivers adapted for the purpose and specially designed CRPL receivers. The receivers presently in service employ a linear detector; however, these are being replaced by new receivers employing a square-law device that will respond to noise power. The detector output is averaged over a period of several minutes by

means of a resistance-capacitance circuit. The averaged detector output voltage operates the automatic-gain-control circuit and a recording meter in such a way as to provide approximately equal decibel intervals on the meter scale with practically any desired dynamic range.

The basic calibration of the equipment is by means of a noise diode. This provides a reference level of available power per unit bandwidth from individual dummy antennas that have been adjusted to match the antenna impedance at each operating frequency. Levels above and below the reference level are calibrated by means of a signal generator through the same dummy antenna. The losses in the antenna are taken into account and the recorded noise level is then expressed in terms of the antenna external noise figure, f_a, which has been defined by Norton [6] as

$$f_a = \frac{p_n}{kt_0 b} \qquad (15)$$

where

p_n = average noise power in watts available from an equivalent lossless antenna.

$kt_0 b$ = noise power in watts available from a passive resistance at reference temperature.

For received noise such as galactic noise having the same amplitude-time distribution as the noise from the calibrating diode, f_a is evaluated as follows:

For equal detector voltages, the noise power, p_a, from the actual antenna (as contrasted to a lossless antenna) is equal to the noise power, p_d, from the calibrating noise diode (since the dummy antenna has been adjusted to the antenna impedance), and this power is given by

$$p_a = p_d = \frac{e i_d r_d b}{2} + kt_d b, \qquad (16)$$

where

e = electronic charge = 1.6018×10^{-19} coulomb [7]

i_d = diode current in amperes

r_d = diode load resistance in ohms

t_d = temperature of diode load resistance in degrees Kelvin.

Taking $t_d = t_0$ (16) becomes

$$p_a = p_d \cong (20 i_d r_d + 1) kt_0 b. \qquad (16a)$$

Expressing the losses in the antenna circuit by a noise figure f_c (see eq (5), sec. 2), the effective noise figure, f_{ac}, for the antenna and antenna losses (taking $t_c = t_0$) is

$$f_{ac} = f_a - 1 + f_c \qquad (17)$$

As the power output of a network is equal to the product of its power gain, noise figure, and $kt_0 b$, then

$$p_a = \frac{(f_a - 1 + f_c) kt_0 b}{fc} \qquad (18)$$

9

Solving (16a) and (18)

$$f_a = 20i_d r_a f_c + 1. \tag{19}$$

Atmospheric radio noise from the antenna and thermal noise from the calibrating noise diode do not have the same voltage distributions with time, and thus for the same average power will not produce the same average output from a linear detector. As f_a is by definition proportional to average power, it is necessary to take into account the effect of the detector in evaluating the measurements.

Landon [19] has shown that the instantaneous voltage of thermal or fluctuation noise follows a normal distribution. Thus in the output of any linear network containing fluctuation noise, the probability that the noise voltage will be between v and $v+dv$ is given by

$$dp = \frac{1}{e\sqrt{2\pi}} \exp\left(\frac{-v^2}{2e^2}\right) dv, \tag{20}$$

where e is the rms noise voltage. When the noise is fed to a linear detector that follows the envelope of the noise, the instantaneous output of the detector will follow a Rayleigh distribution [20]. The probability that the instantaneous output voltage lies between a and $a+da$ is

$$dp_a = \frac{a}{e^2} \exp\left(\frac{-a^2}{2e^2}\right) da. \tag{21}$$

The average detector output voltage, $\bar{a}$ that would be measured with a long time constant record is the integral form $a=0$ to ∞ of adp_a. Thus

$$\bar{a} = \int_0^\infty \frac{a^2}{e^2} \exp\left(\frac{-a^2}{2e^2}\right) da = \sqrt{\pi/2} = 1.253e. \tag{22}$$

If the recorder were calibrated by substituting a sine-wave signal for the thermal noise and adjusting its intensity to give the same recorder deflection, the recorder voltages would be

$$a_s = e_s\sqrt{2} = 1.414\, e_s, \tag{23}$$

where

a_s = detector output voltage with sine-wave input
e_s = rms voltage of sine-wave input to detector.

As the sine-wave input was adjusted so that $a_s = \bar{a}$, the rms noise voltage is

$$e = 1.129\, e_s. \tag{24}$$

Atmospheric noise does not lend itself readily to mathematical analysis because it does not follow any specified distribution. Therefore, it is necessary to use experimental methods to determine the effect of the detector characteristics on the recorded noise. Jansky [21] has stated that, from his experimental measurements, the ratio of average to effective voltage is 0.85 for thermal noise and 0.55 to 0.8 for atmospheric. From his circuit diagram, it appears that he was measuring the average value of the noise envelope instead of the average value of the noise. The latter was defined by Jansky to be the average of the instantaneous noise values without regard to sign. It was shown theoretically in (24) that when thermal noise is measured with a linear detector, calibrated with a sine-wave signal, the ratio of rms sine-wave voltage to the rms noise voltage is 0.886. This theoretical factor apparently corresponds to Jansky's experimental value of 0.85 for thermal noise, and thus the ratio of rms sine-wave voltage to rms atmospheric noise voltage has been assumed to fall between Jansky's measured values of 0.55 to 0.8. Using the geometric mean of these two limiting values, the rms atmospheric noise voltage will be $1.51\, e_s$, where e_s is the rms sine-wave carrier voltage used to calibrate the linear detector.

Recent measurements at CRPL, using both a square law and linear detector, have indicated that the above ratio is 3.1 on 50 kc and 1.55 on 2.5 Mc. However, besause of the limited number of CRPL observations, Jansky's ratio of 1.51 has been used in analyzing all of the atmospheric-noise data for this paper.

As calibration of the CRPL noise recorders is by means of a noise diode instead of a sine-wave signal, it is necessary to combine Jansky's factor of 1.51 with the factor obtained from (24), and thus the average atmospheric noise power from the actual antenna is given by

$$p_a = \left(\frac{1.51}{1.129}\right)^2 p_d = 1.79\, p_d, \tag{25}$$

and for atmospheric noise powers greater than about $10\, kt_0 b$,

$$f_a = 35.8\, i_d r_a f_c. \tag{26}$$

Thus, F_a, in decibels, above $kt_0 b$, is

$$F_a = I_d + R_d + F_c + 15.54, \tag{27}$$

where
$I_d = 10\log_{10} i_d$, $R_d = 10\log_{10} r_d$, $F_c = 10\log_{10} f_c$, provided the resulting value of F_a is greater than 10.

Measurements of radio noise levels at Tatsfield, England, were made by means of the Thomas method of subjective observations in which an operator adjusts the level of a low-speed radio-telegraph signal relative to the received noise so that about 95-percent copy is obtained. The noise is received on a short vertical antenna, and the data are reported in terms of the minimum required signal field strength, f_m, expressed in microvolts per meter. Taking the CCIR [17] required signal-to-noise ratio of -7 db for a bandwidth of 6 kc for 90-percent intelligibility of 8 baud, low grade, A1 telegraphy, the noise field strength, f_n, in microvolts per meter, is

$$f_n = 2.24 f_m. \tag{28}$$

The lossless-antenna noise power, in watts, is

$$p_n = \frac{f_n^2 h_e^2}{4r_a} (10^{-12}) \tag{29}$$

where

h_e = effective height of the antenna in meters = ½ actual height, h.

r_a = radiation resistance in ohms = $40\pi^2(h/\lambda)^2$.

From (28) and (29), and taking into account the ground-wave antenna power gain, g_m, relative to a short vertical monopole, f_a for the Tatsfield measurements is

$$f_a = (1.305)(10^{-18})\frac{f_m^2\lambda^2}{\pi^2 kt_0}\,g_m = (2.871)(10^6)\frac{f_m^2}{f_{Mc}^2}\,g_m \quad (30)$$

where

f_m = required signal field strength in microvolts per meter

f_{Mc} = frequency in megacycles.

Thus F_a, in decibels above kt_0b, is

$$F_a = F_m + G_m - 20\,\log_{10} f_{Mc} + 64.58, \quad (31)$$

where

$$F_m = 20\,\log_{10} f_m$$

$$G_m = 10\,\log_{10} g_m.$$

8. Appendix 2. Analysis

This paper includes the analysis of:

1. A year's data of 145 kc and 2.5 Mc at Boulder, Colo. (June 1952 through May 1953).

2. A year's data of 135, 535, and 2,180 kc from Front Royal, Va. (June 1952 through May 1953).

3. A week of 50-kc average power measurements at Boulder, Colo. (June 1 through 7, 1953).

4. Part of a year's data of 5, 10, and 20 Mc from Front Royal, Va. (September 1952 through May 1953).

5. A year's data of 2.5, 5, 10, 15, and 20 Mc from Tatsfield, England (March 1952 through February 1953).

6. Eight days of galactic radio noise of 10 and 20 Mc at Boulder, Colo. (June 12, 1953 through June 19, 1953).

The analysis of the Boulder radio-noise data at 50 kc, 145 kc, and 2.5 Mc consisted of editing to remove erratic data, tabulating hourly medians, and preparing cumulative distributions.

The editing was done by comparing the frequency records day by day and hour by hour in order to find signal contamination, inspecting each frequency for abrupt gain changes, and by inspecting daily calibrations to find changes that would result in errors larger than 2 db. If any portion of adjacent calibrations differed by more than 4 db, the record between the calibration was deleted, but if the difference was less than 4 db, the record was retained and the tabulation made by using the first calibration to the middle of the interval between calibrations and the second calibration for the second half of the interval.

The tabulations were for hourly medians of the recorded chart when no signal was present, but if a minor signal contamination was present, the median of the bottom of the trace was recorded. The data were tabulated in decibels above the reference noise diode level, and the results of the analysis were converted to F_a in decibels above kt_0b by adding the appropriate correction (see appendix 1).

Cumulative amplitude-time distributions were obtained for each time block, which included data for 4 hours of each day during a whole season. Thus there were approximately 360 possible hourly values in each time block with 6 time blocks for each season at a given station and frequency. The time blocks began at midnight and included data from 0000 to 0400, 0400 to 0800, etc.

The Front Royal data listed as items 2 and 4 were analyzed in the same manner, except that additional frequencies enabled a more thorough search for contaminating signal, as there were at least two frequencies in operation all of the time.

The Tatsfield, England, data were received in tabulated form, and thus could not be subjected to the same editing procedure as the Boulder and Front Royal data. However, as they were obtained by subjective methods, they were not likely to contain signal contamination. These data, after being converted to values of F_a (see appendix 1), were analyzed in a similar manner for the same time blocks.

The cumulative distributions for the time blocks were used in a study of their slopes as a function of their median magnitudes. Ratios of upper deciles to medians and medians to lower deciles averaged by 10-db intervals were plotted as functions of the corresponding median radio noise levels. These two curves are shown in figure 32.

In addition, average ratios of upper deciles to medians and medians to lower deciles of radio noise levels were plotted as a function of frequency and time blocks and smooth curves drawn. See figure 33.

The galactic radio-noise analysis, listed as item 6 above, is discussed in appendix 4.

As a measure of manmade radio noise, the medians at 535 kc, 2.5 Mc, and 5 Mc for time block 0800 to 1200 were averaged for each frequency and a straight line drawn through the points plotted on semilog paper. The straight line went through all three points. This line was used as representing manmade radio noise. See Predictions, appendix 3. An average ratio of upper deciles to medians gave a 9.3-db value, and an average ratio of medians to lower decile gave a 9.4-db value.

9. Appendix 3. Predictions

The atmospheric radio-noise prediction curves in National Bureau of Standards Circular 462 were modified by:

1. Averaging the curves that bounded each 4-hour time block.

2. Converting to the upper decile value of F_a.
3. Changing from upper decile of F_a to median F_{am}.
4. Extrapolating to 10 kc.
5. Adding lines representing manmade noise.
6. Correcting galactic radio noise levels.

Data presented in this paper are for 4-hour time blocks centered on 0200, 0600, 1000, 1400, 1800, and 2200. Thus it was necessary to modify the curves in NBS Circular 462 by averaging the curves bounding time blocks.

The curves in Circular 462 are in terms of minimum required carrier field intensities, f_s, to assure radio-telephone communication 90 percent of the time in the presence of atmospheric and galactic noise. Taking the CCIR [17] required peak signal-to-noise ratio of 15 db for a bandwidth of 6 kc for A3 double sideband low-grade telephoney, and subtracting 6 db to obtain the carrier signal-to-noise ratio, the upper decile noise field strength, f_n, in microvolts per meter, is

$$f_n = 0.355 \, f_s. \tag{32}$$

From eq (32) and (29) of appendix 1, and following the method used in appendix 1 on Tatsfield data, the upper decile value of f_a for the NBS Circular 462 field-strength curves is

$$f_a = 3.28 \times 10^{-20} \frac{f_s^2 \lambda^2}{\pi^2 kt} g_m = 7.28 \times 10^4 \frac{f_s^2}{f_{Mc}^2} g_m. \tag{33}$$

Thus F_{am}, in decibels above $kt_0 b$, is

$$F_{am} = F_s + G_m - D_u - 20 \, \log_{10} f_{Mc} + 48.6 \tag{34}$$

where
$F_s = 20 \, \log_{10} f_s$
$G_m = 10 \, \log_{10} g_m$
$D_u =$ the ratio of the upper decile to median value, as given in figure 33.

Measurements made at the University of Florida [22] for low-frequency radio noise were used to extrapolate the prediction curves below 100 kc. This was done by blending measurements made at Gainesville, Fla., with the prediction curve values at 100 kc. The Florida data were reported in decibels above 1 μv/m for a 1-kc bandwidth. Correction factors were applied to change this to decibels above $kt_0 b$.

In addition to the atmospheric radio noise prediction curves, lines representing manmade noise and galactic noise were drawn in. The galactic radio noise is discussed in appendix 4. The man-made radio noise line used was determined by assuming that the 8 to 12 o'clock measurements of 535 kc, 2.5 Mc, and 5 Mc at Boulder, Front Royal, and Tatsfield, respectively, represent primarily manmade noise. Obviously this line may only be used when similarly quiet locations are being considered. The average ratio of upper decile to median values for the manmade noise for the three stations was found to be 9.3 db, and the average ratio of median to lower deciles was found to be 9.4 db.

10. Appendix 4. Galactic Radio Noise

Galactic radio noise is not of uniform intensity from all points in the celestial sphere but varies with direction. Because the zenith of a vertical whip antenna would be a function of time and latitude, the galactic noise received would be a function of time and latitude also. In order to find how galactic radio noise varies with the latitude and local time of an observer, an integration of the known sources of galactic radio noise was carried out. The galactic radio noise power, F_a, expressed in decibels above $kt_0 b$, is given by [23]

$$F_a = 10 \, \log_{10} \left[\frac{\lambda^2 \iint_{4\pi} i(\theta, \phi) \, g_i(\theta, \phi) \, d\omega}{4\pi kt} \right], \tag{35}$$

where
$\lambda =$ the wavelength in meters
$i(\theta, \phi) =$ the incident intensity of galactic radio noise from the direction, (θ, ϕ)
$g_i(\theta, \phi) =$ the antenna gain in the direction, (θ, ϕ), relative to an isotropic antenna
$d\omega =$ the element of solid angle.

In actual practice, the following numerical integration was used:

$$F_a = 10 \, \log_{10} [c + d \sum rg \cos \phi] - 10 \, \log_{10} kt_0, \tag{36}$$

where
$r =$ a number proportional to the galactic radio noise intensity from 10° by 10° areas of the celestial sphere
$g =$ the relative antenna gain averaged over the same area
$\phi =$ the average celestial latitude of the area
d and $c =$ constants obtained through the adjustment of the final integrated curves in such a manner that they agree with the Boulder measurements at 40° N latitude.

From the information obtained through this summation, it was possible to plot graphs of galactic radio noise intensity versus the local time and latitude of the observer.

The numbers, r, assigned to areas of the celestial sphere were approximately proportional to the galactic radio noise intensity and were abstracted from Reber's [9, 10, 11, 12] galactic radio-noise map and from a similar map for the southern sky constructed by Bolton and Westfold [24]. The numbers, r, are the average Reber contours for the 10° by 10° areas of the celestial sphere. These contours were extended to the southern hemisphere by a qualitative extrapolation of Reber's contours consistent with the results of Bolton and Westfold. Although Reber's contours are indicative of the galactic radio-noise intensities emanating from the various portions of the sky, they were determined by means of an antenna with a rather wide beam, and, therefore, do not represent the exact distribution of noise intensity in the sky. Also, they were

measured at 160 Mc, and, therefore, do not represent absolute intensities at 20 Mc, for which the integration was performed. Reber assumed that the galactic radio noise intensity from the dark or "cold" portions of the sky was zero. More recent measurements, however, have shown that some energy does emanate from the whole sky. Therefore, the final results of the integration were adjusted by means of the constants c and d to agree with actual measurements at 40° latitude at 20 Mc.

The antenna gain pattern from which the numbers, g, were calculated, was obtained from [18]. The antenna pattern used was one for a vertical half-wave antenna over good ground at 20 Mc.

The entire integration was carried out for a frequency of 20 Mc. However, it can be extended to any frequency by using the frequency law for galactic radio noise obtained from measurements made on horizontally polarized antennas by Cottony and Johler [25]. Integrations were made at 4-hour intervals during the sidereal day for latitudes ranging from 80° N to 80° S in 20° steps. The integration at 40° N was forced to fit data obtained at Boulder, Colo., 40° N, thus determining the constants c and d of eq (36). The maximum and minimum of the summations $\Sigma rg \cos \phi$ for 40° N were 2789 and 414, respectively. The maximum and minimum values of F_a for the Boulder measurements were 24 and 21 db, respectively. The constants determined from the above values are therefore $c=4.35\times10^{-19}$ watts per cycle and $d=2.17\times10^{-22}$. The constant c was found to represent an effective blackbody temperature of 31,500 K at 20 Mc for the dark portions of the sky. Applying the frequency law, $t \alpha f^{-2.3}$, we find that this constant represents a temperature of 778° K at 100 Mc, a result in good agreement with Bolton and Westfold for the dark portions of the sky.

The galactic radio noise measurements were made at Boulder, Colo., with the standard atmospheric radio-noise measuring equipment described in appendix 1. The equipment was operated with the long time constant removed, and, in addition, the lowest values for each hour were taken from data covering several days of operation. These two precautions made the effects of atmospheric and manmade radio noise negligible.

From the integration and forced fit to the measurements at 40° N latitude, the other integrations at the rest of the latitudes were put on an absolute basis. (See fig. 41.)

Because sidereal time gains on solar time by 6 hours each season, it was possible to compute the upper and lower deciles and the median values of galactic radio noise levels during 4-hour time blocks by season in a fashion identical with that followed in the analysis of atmospheric radio noise (see fig. 43).

11. References

[1] H. A. Thomas and R. E. Burgess, Survey of existing information and data on atmospheric noise level over the frequency range 1–30 Mc/s, Radio Research Board Paper R. R. B./C. 90 (Radio Division, National Physical Laboratory, Teddington, England, Feb. 21, 1944).

[2] IRPL radio propagation handbook (Dept. of Comm., National Bureau of Standards, Nov. 1943).

[3] Minimum required field intensities for intelligible reception of radio telephony in presence of atmospherics or receiving set noise, Radio Prop. Unit Tech. Rept. 5, 1st ed. (Holabird Signal Depot, Baltimore, Md., Dec. 1945).

[4] Ionospheric radio propagation, NBS Circular 462 (Supt. of Doc., Washington, D. C., 1948). $1.00.

[5] H. T. Friis, Noise figure of radio receivers, Proc. IRE **32**, 419 (1944).

[6] Kenneth A. Norton, Transmission loss in radio propagation, Proc. IRE **41**, 146 (1953).

[7] J. A. Bearden, H. M. Watt, A re-evaluation of the fundamental atomic constants, Phys. Rev. [1] **81**, 73 (1951).

[8] S. A. Schelkunoff, Electromagnetic waves (D. Van Nostrand Co., Inc., New York, N. Y., 1943).

[9] G. Reber, Cosmic static, Proc. IRE **28**, 68 (1940).

[10] G. Reber, Cosmic static, Proc. IRE **30**, 367 (1942).

[11] G. Reber, Cosmic static, Astrophys. J. **100**, 279 (1944).

[12] G. Reber, Cosmic static, Proc. IRE **36**, 1215 (1948).

[13] Lord Rayleigh, On the resultant of a large number of vibrations of the same pitch and of arbitrary phase, Phil. Mag. **10**, 73 (1880) and **27**, 460 (1889). See also the book "Theory of sound" (1894) 2d ed., par. 42a, or Sci. Papers, I, 491, On the problem of random vibrations and of random flights in 1, 2, or 3 dimensions, Sci. Papers, I, 604.

[14] Newbern Smith and M. B. Harrington, The variability of sky-wave field intensities at medium and high frequencies, (Unpublished NBS report).

[15] Report of the Ad Hoc Committee for the evaluation of the radio propagation factors concerning the television and frequency modulation broadcasting services in the frequency range between 50 and 250 Mc, Fed. Communications Comm. Mimeo. Numbers 36728 (May 26, 1949), 36830 (May 31, 1949), and 54382 (July 7, 1950).

[16] Ground wave field intensities, Radio Prop. Unit Tech. Rept. 3, revised June 1949 (Baltimore Signal Depot, Baltimore, Md).

[17] Bandwidths and signal-to-noise ratios in complete systems, CCIR, VI Plenary Assembly, International Radio Consultative Committee **1**, 30 (Geneva, 1951).

[18] Radiations from antennas in the 2 to 30 magacycle band, Radio Prop. Unit Tech. Rept. 2, 61 (Baltimore Signal Depot, Baltimore, Md., July 1947).

[19] Vernon D. Landon, The distribution of amplitude with time in fluctuation noise, Proc. IRE **29**, 50 (1941).

[20] Kenneth A. Norton, Discussion of reference [19], Proc. IRE **30**, 425 (1942), and Corrections, p. 526 (Nov. 1942).

[21] Karl G. Jansky, An experimental investigation of the characteristics of certain types of noise, Proc. IRE **27**, 763 (1939).

[22] A. W. Sullivan, H. M. VanValkenburg, and J. M. Barney, Low frequency atmospheric radio noise in Florida, Trans. Am. Geophys. Union [3] **33**, 650 (1952).

[23] J. W. Herbstreit, Cosmic radio noise, Advances in Electronics **1**, 347 (1948).

[24] J. G. Bolton and K. C. Westfold, Galactic radiation at radio frequencies, I. 100 Mc/s. Survey, Australian J. Sci. Res., Series A-Phys. Sci. [1] **3**, 19 (1950).

[25] H. V. Cottony and J. R. Johler, Cosmic radio noise intensities in the VHF band, Proc. IRE **40**, 1053 (Sept. 1952).

FIGURE 1. *Network for definition of f, the effective receiver noise figure.*
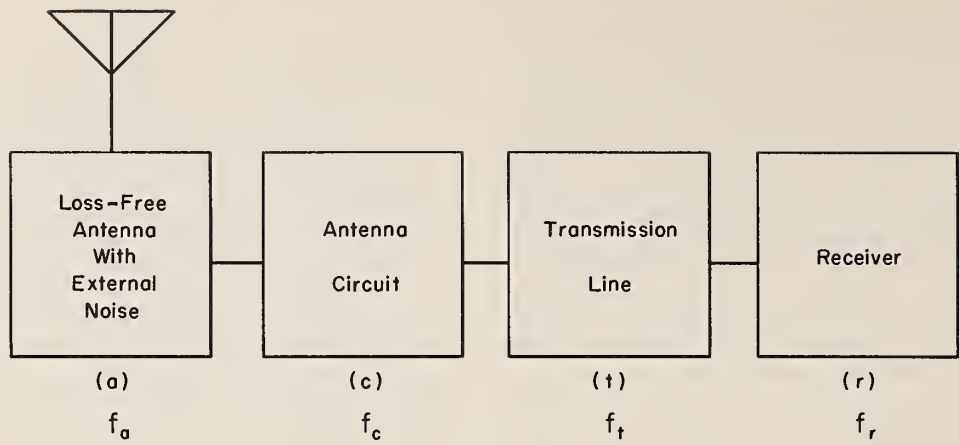
$$f = f_{actr} = f_a - 1 + f_c \, f_t \, f_r$$
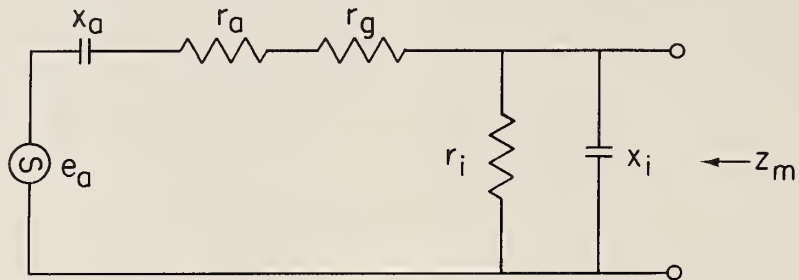

FIGURE 2. *Equivalent antenna circuit.*
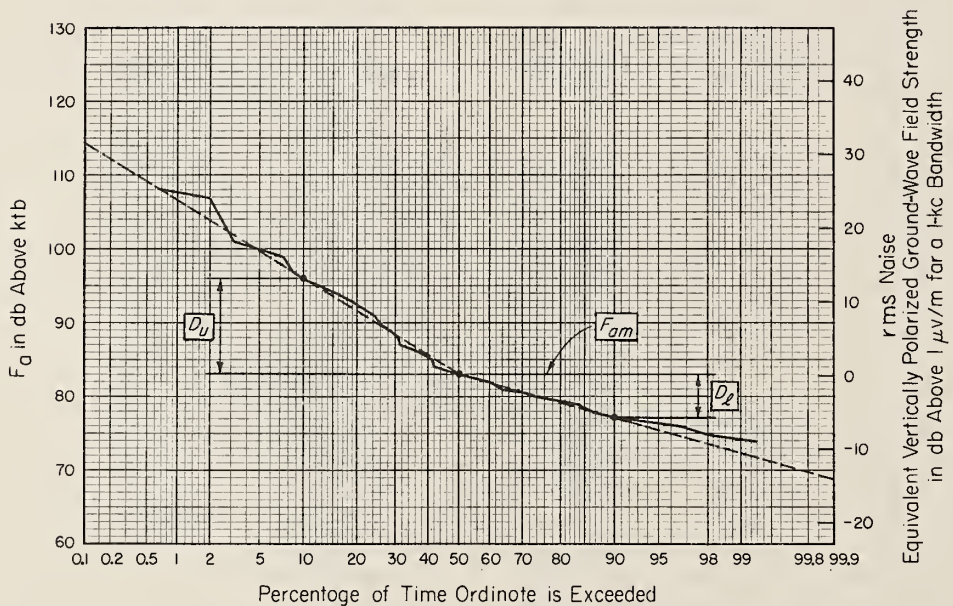
FIGURE 3. *Distribution of hourly medians for Front Royal, Va., 135 kc.*
For the time block, 1200–1600, September–October–November, 1952.
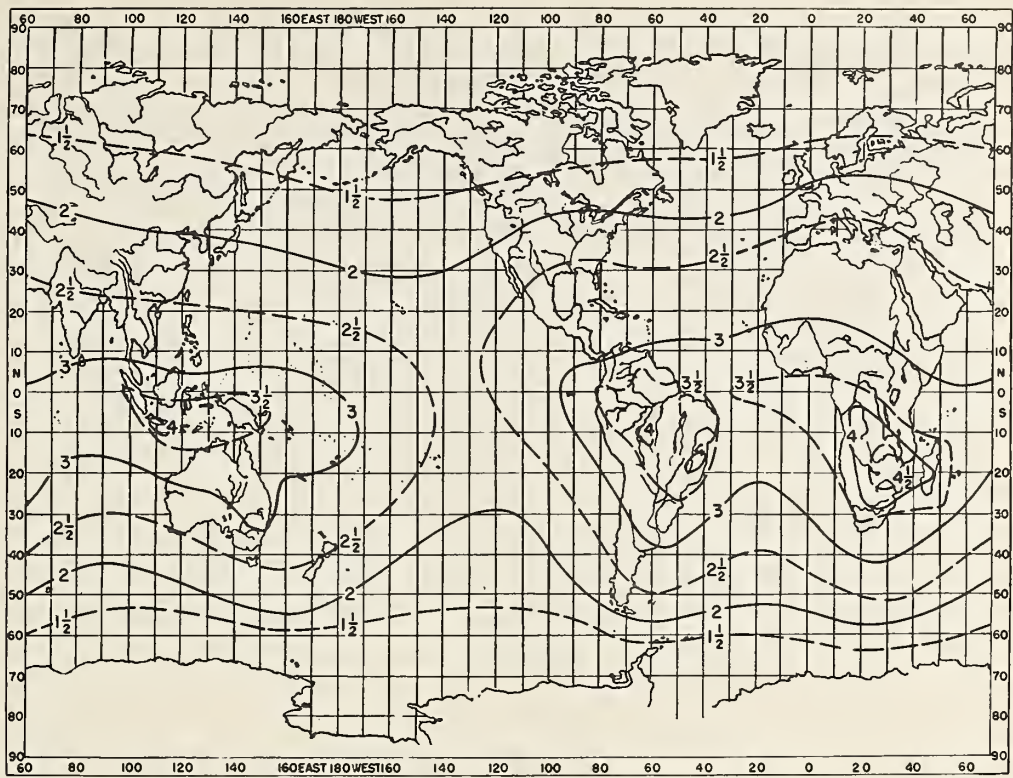
FIGURE 4. *Noise distribution for period December-January-February.*
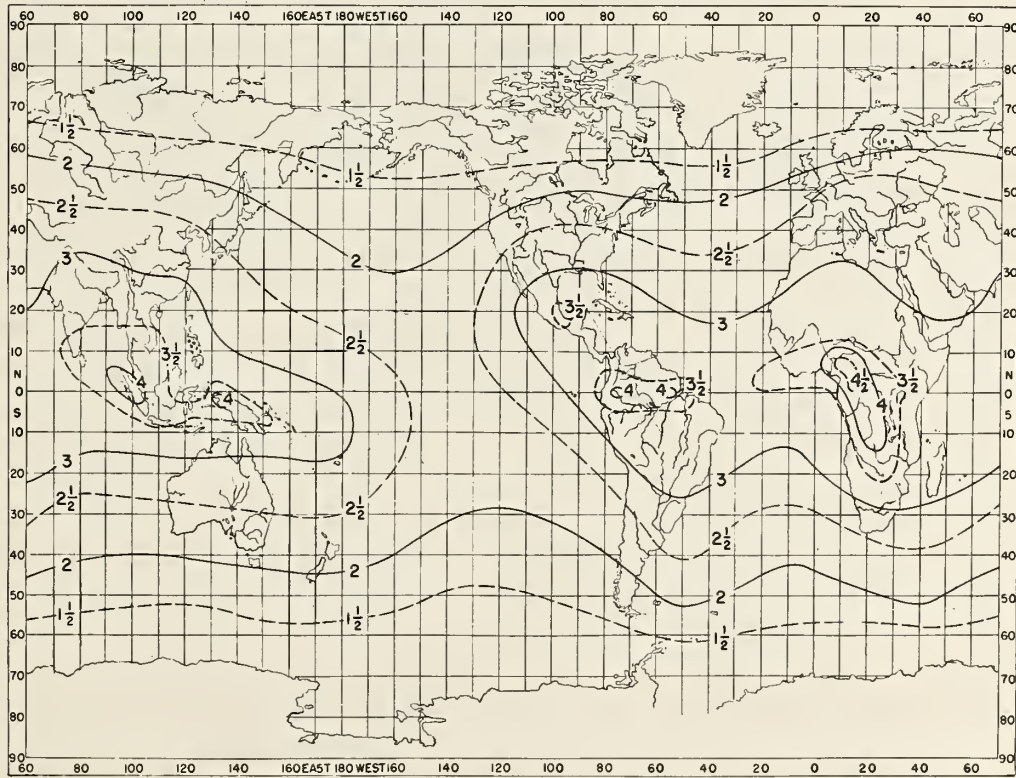
FIGURE 5. *Noise distribution for period March-April-May.*
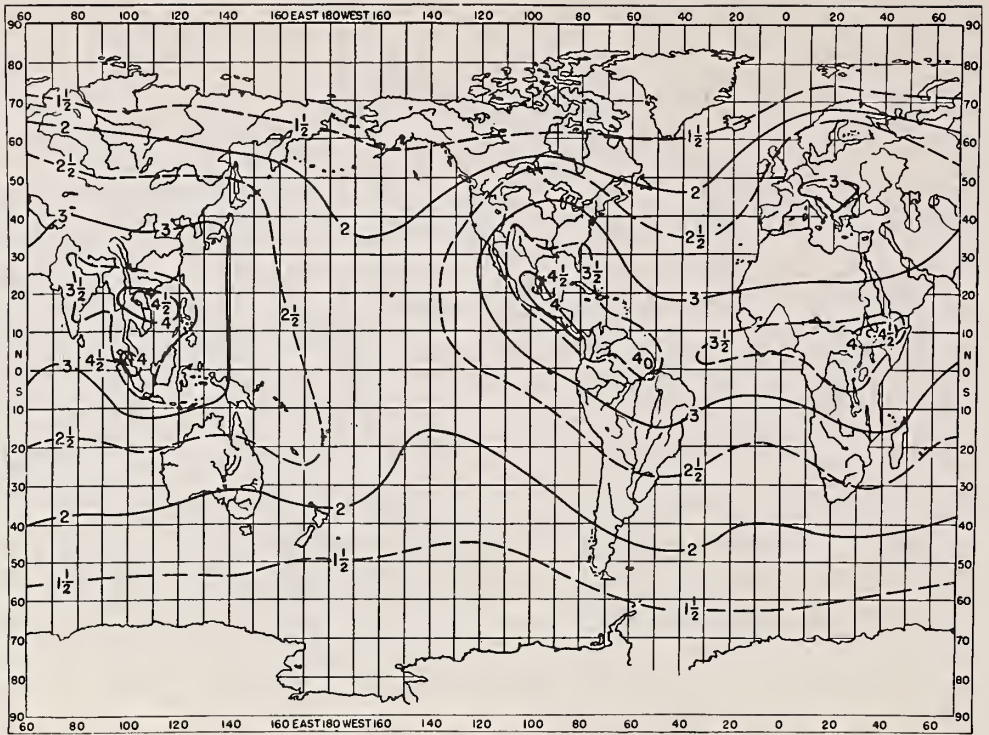
FIGURE 6.   *Noise distribution for period June-July-August.*
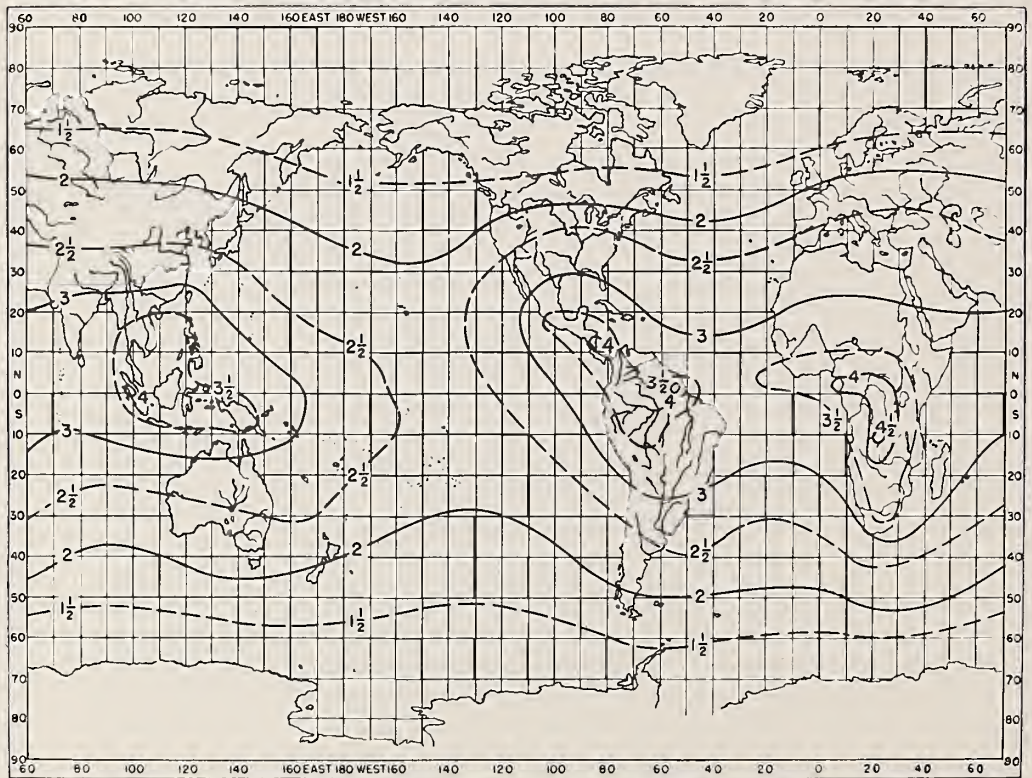
FIGURE 7.   *Noise distribution for period September-October-November.*

16
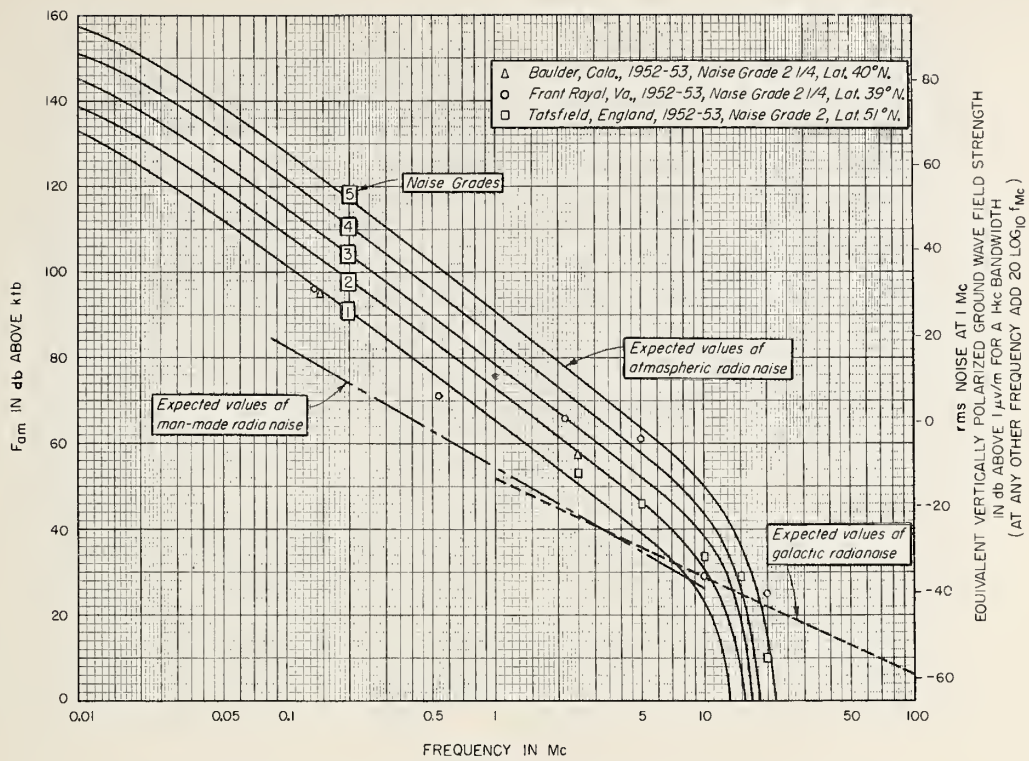
FIGURE 8. *Median values of radio noise expected for a short vertical antenna.*
For the time block, 0000–0400, winter.
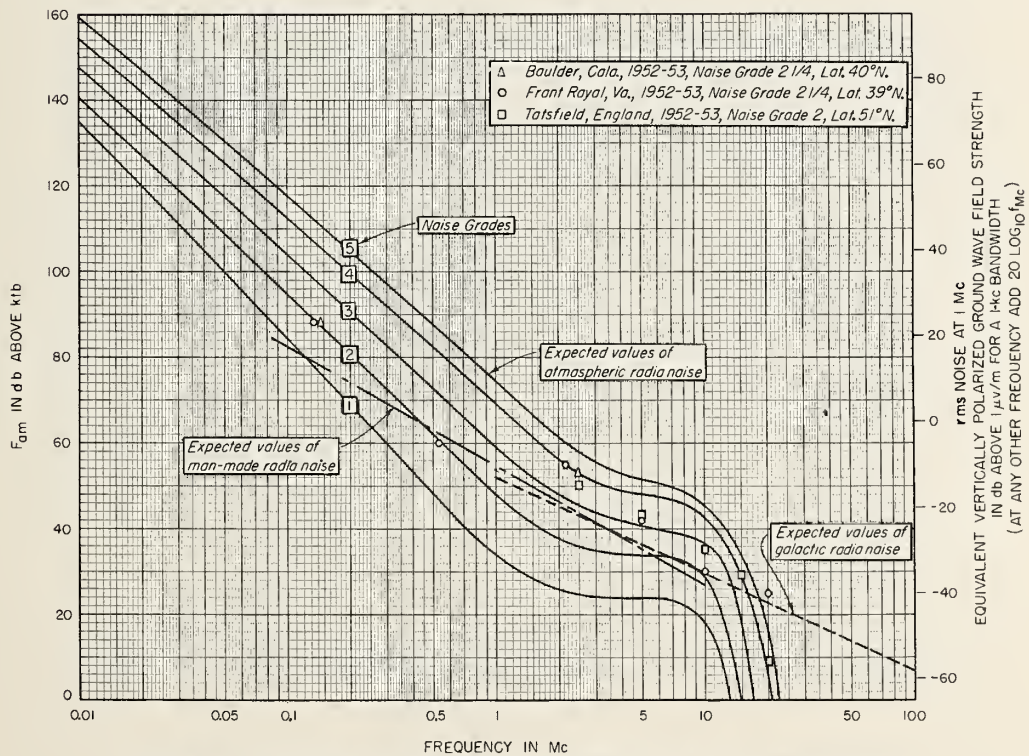
FIGURE 9. *Median values of radio noise expected for a short vertical antenna.*
For the time block, 0400–0800, winter.

17
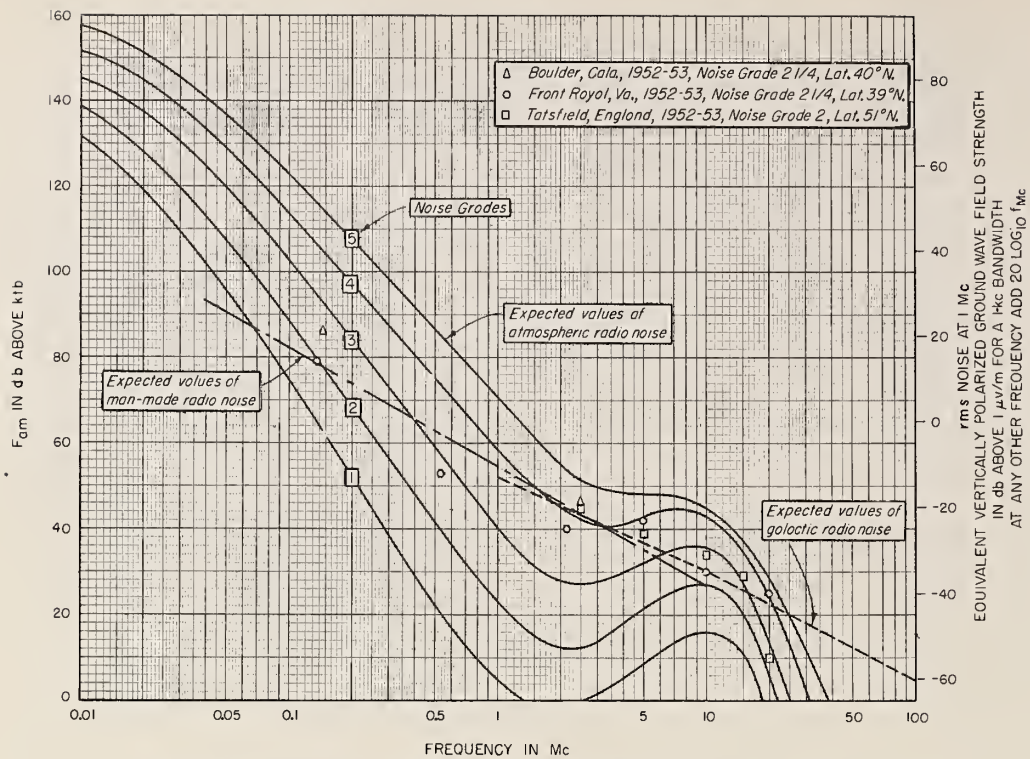
FIGURE 10. *Median values of radio noise expected for a short vertical antenna.*
For the time block, 0800–1200, winter.
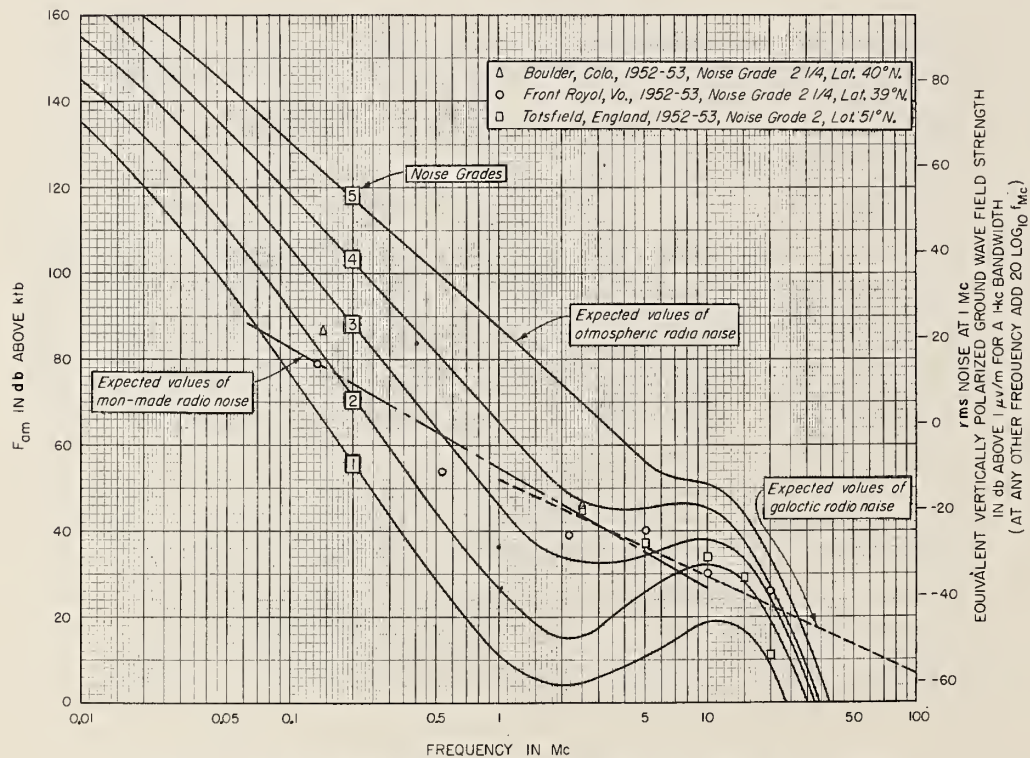
FIGURE 11. *Median values of radio noise expected for a short vertical antenna.*
For the time block, 1200–1600, winter.
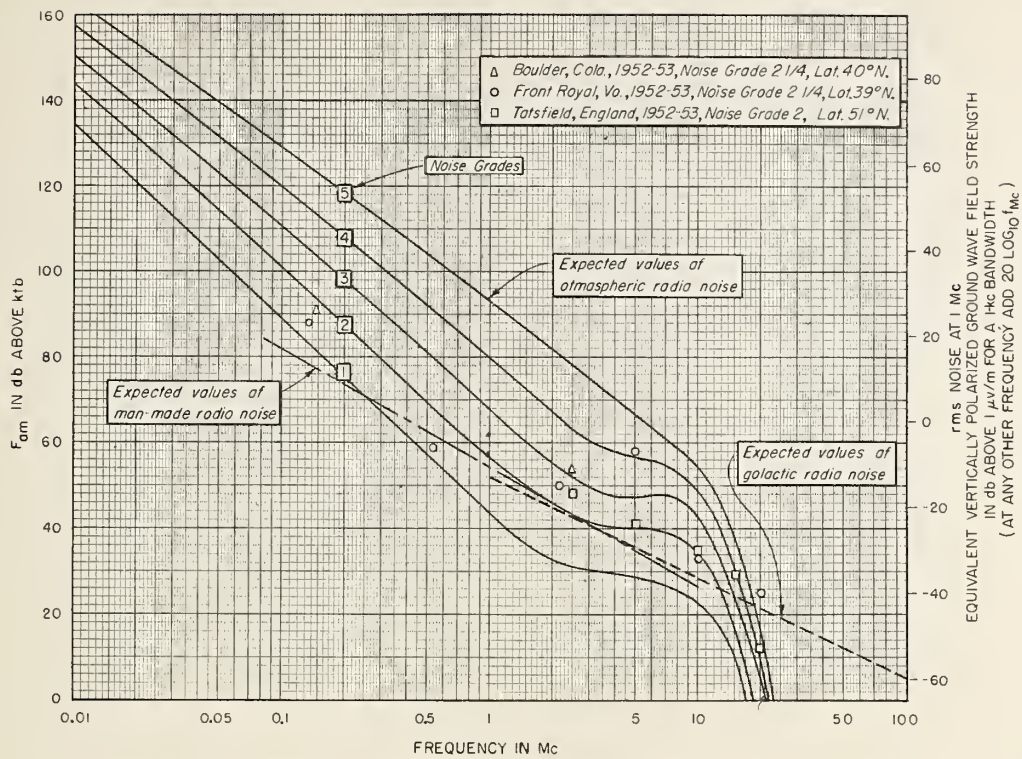
FIGURE 12. *Median values of radio noise expected for a short vertical antenna.*
For the time block, 1600–2000, winter.
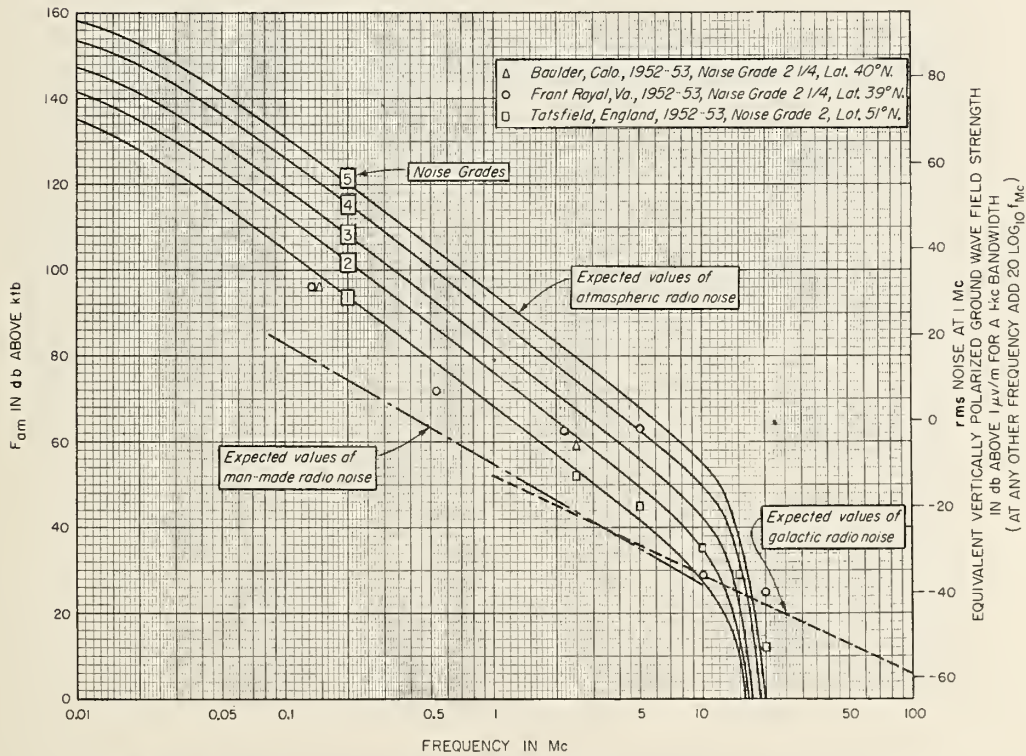
FIGURE 13. *Median values of radio noise expected for a short vertical antenna.*
For the time block, 2000–2400, winter.

19
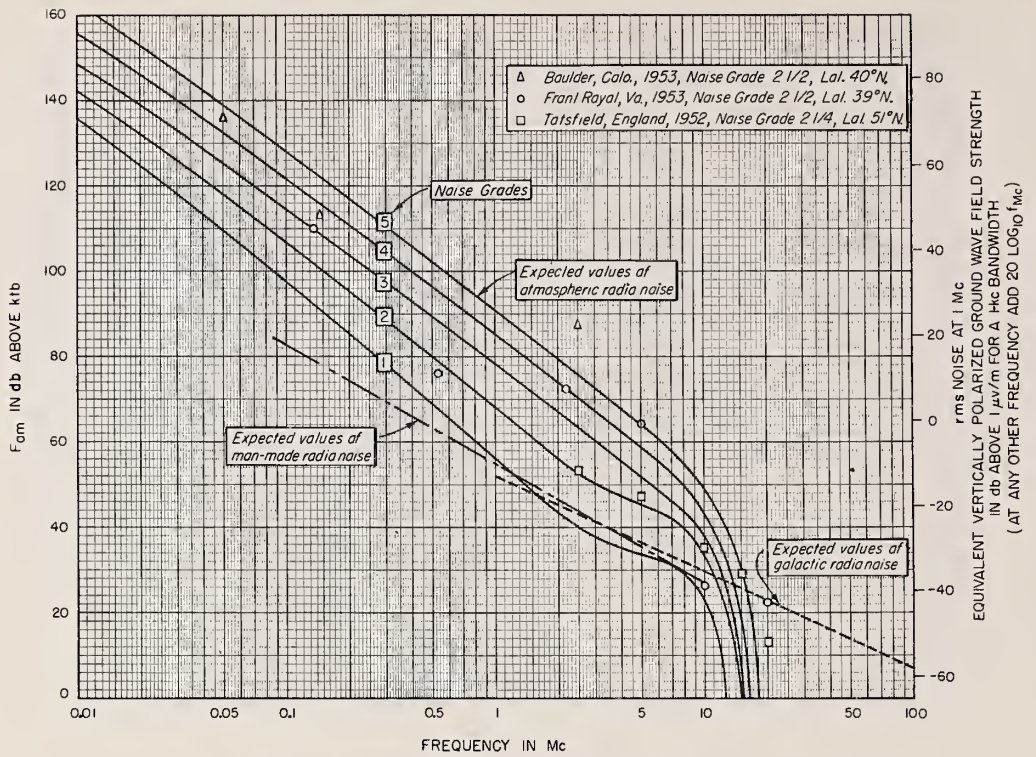
FIGURE 14. *Median values of radio noise expected for a short vertical antenna.*
For the time block, 0000–0400, spring.
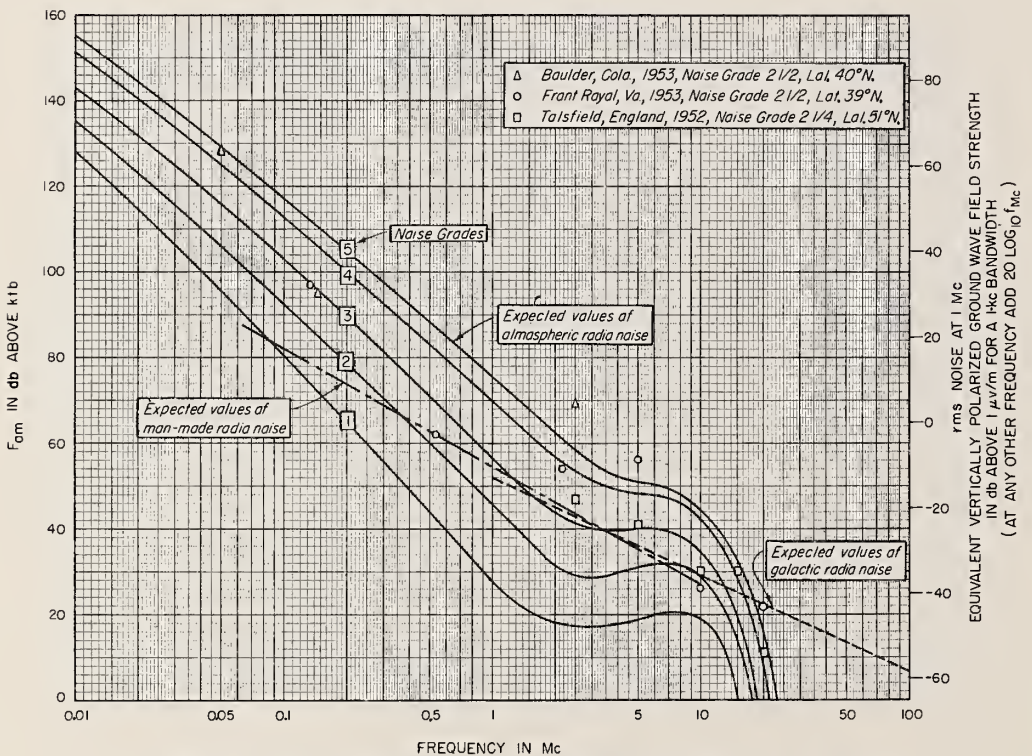
FIGURE 15. *Median values of radio noise expected for a short vertical antenna.*
For the time block, 0400–0800, spring.
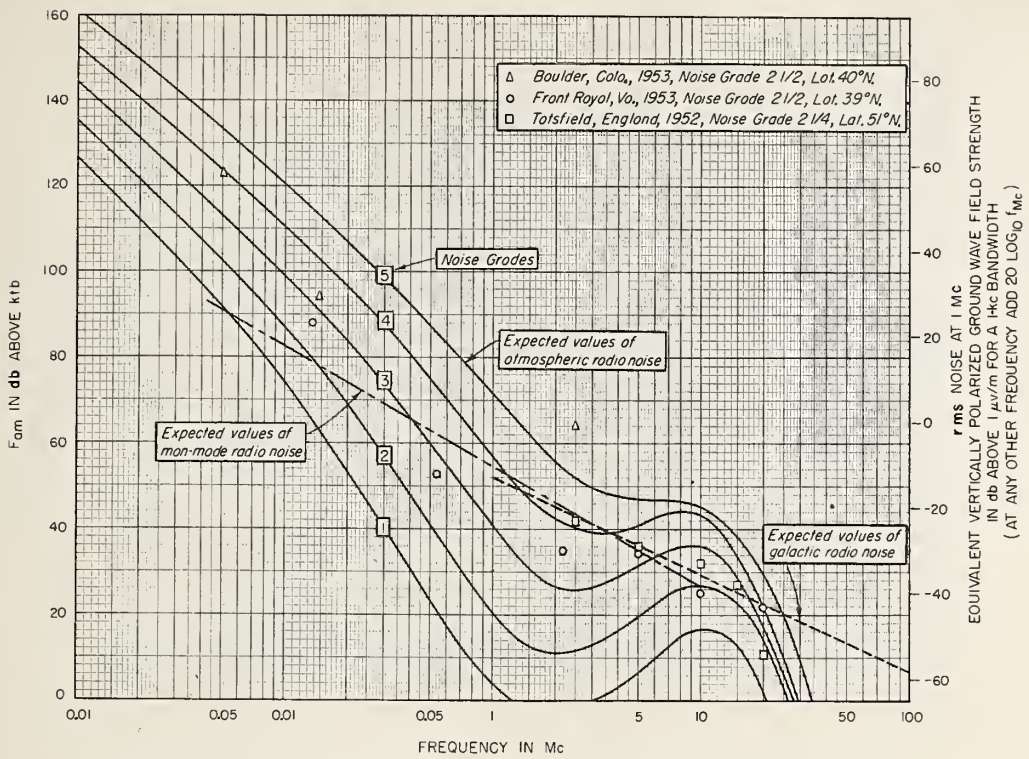
FIGURE 16. *Median values of radio noise expected for a short vertical antenna.*
For the time block, 0800–1200, spring.
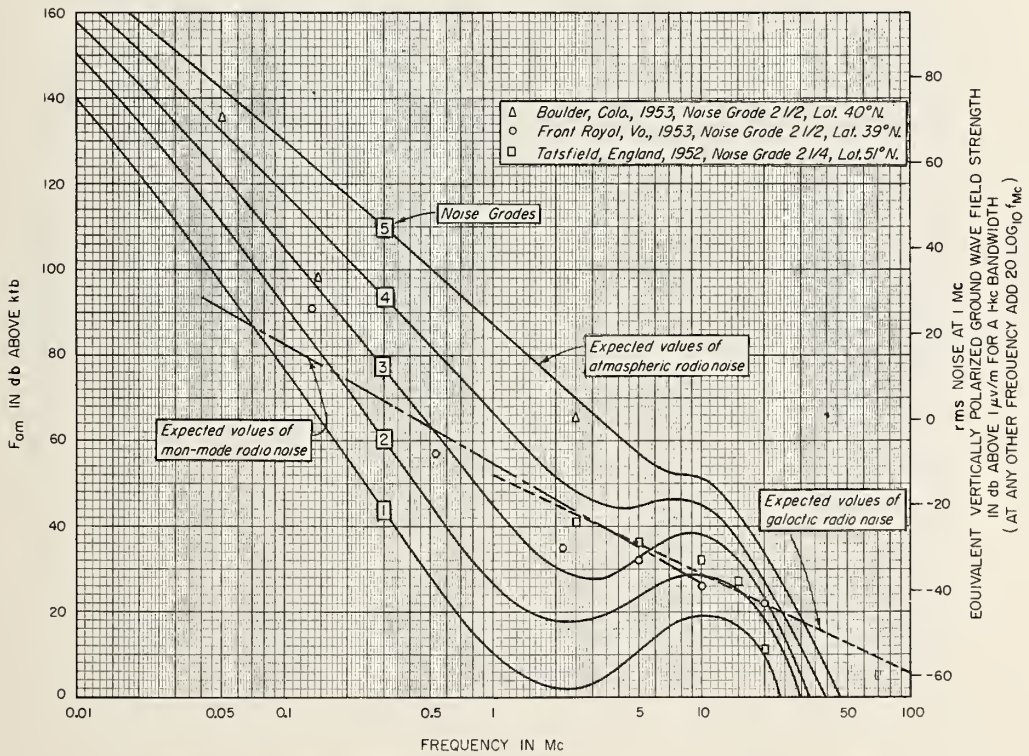
FIGURE 17. *Median values of radio noise expected for a short vertical antenna.*
For the time block, 1200–1600, spring.
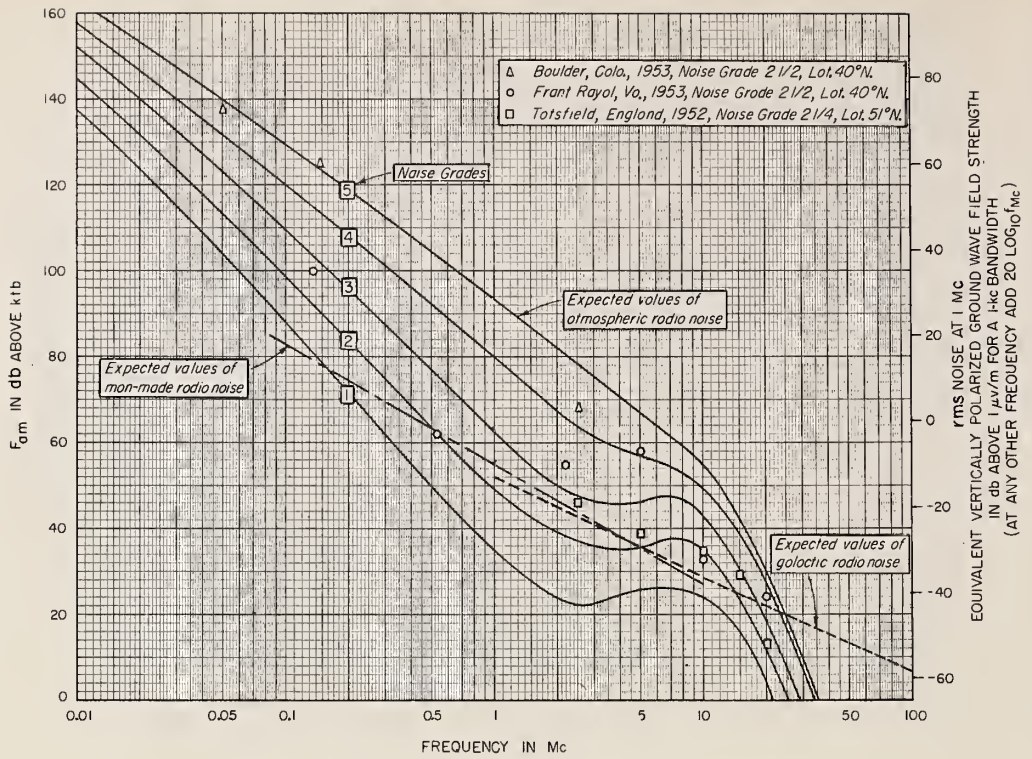
FIGURE 18. *Median values of radio noise expected for a short vertical antenna.*
For the time block, 1600–2000, spring.
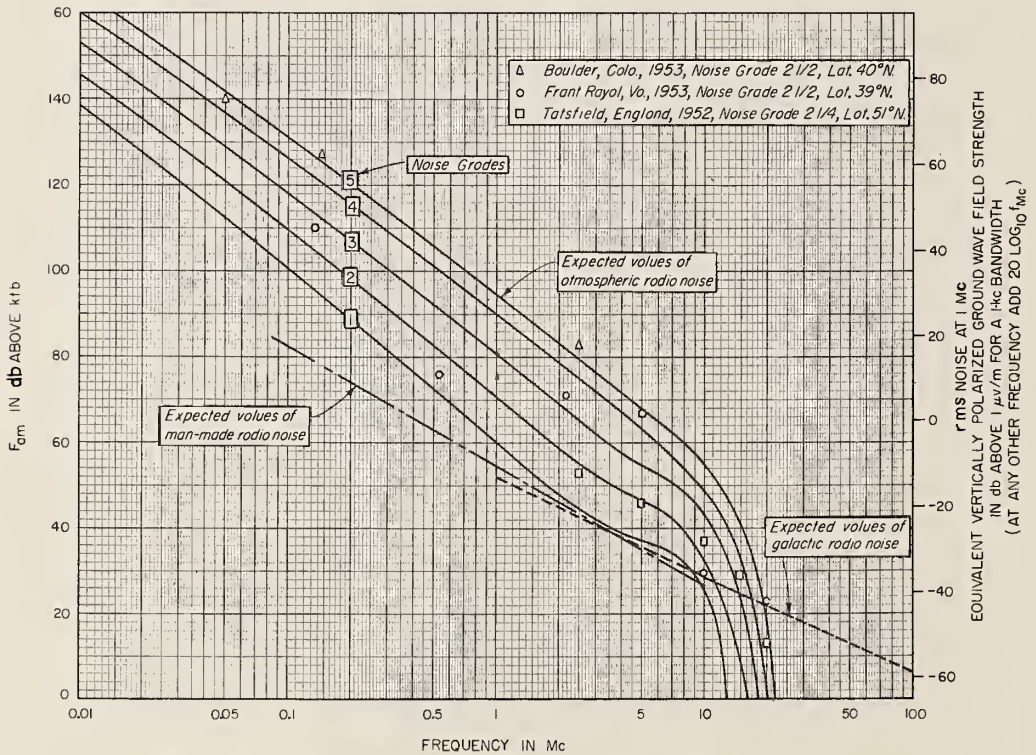
FIGURE 19. *Median values of radio noise expected for a short vertical antenna.*
For the time block, 2000–2400, spring.

22
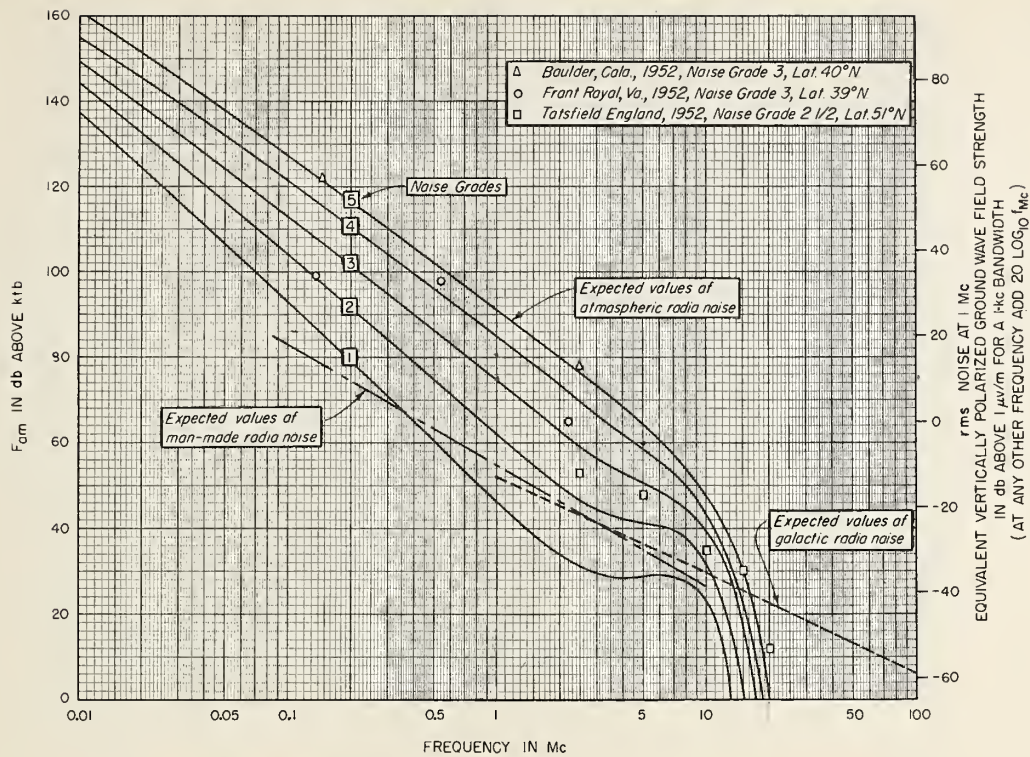
FIGURE 20.   *Median values of radio noise expected for a short vertical antenna.*
For the time block, 0000–0400, summer.
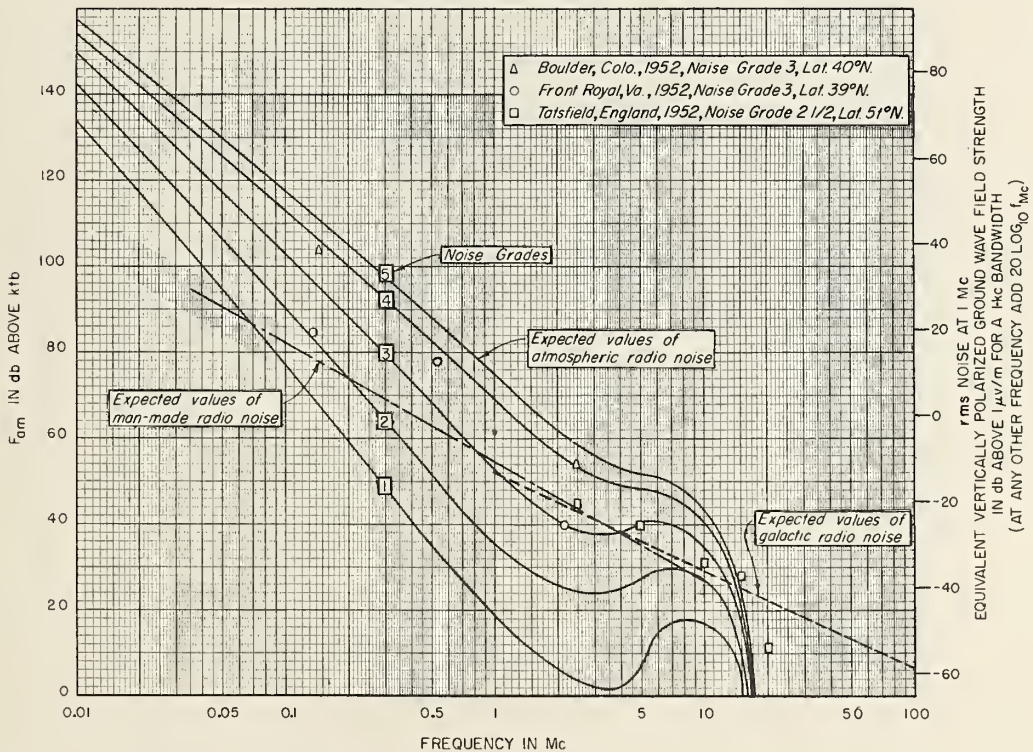
FIGURE 21.   *Median values of radio noise expected for a short vertical antenna.*
For the time block, 0400–0800, summer.

23
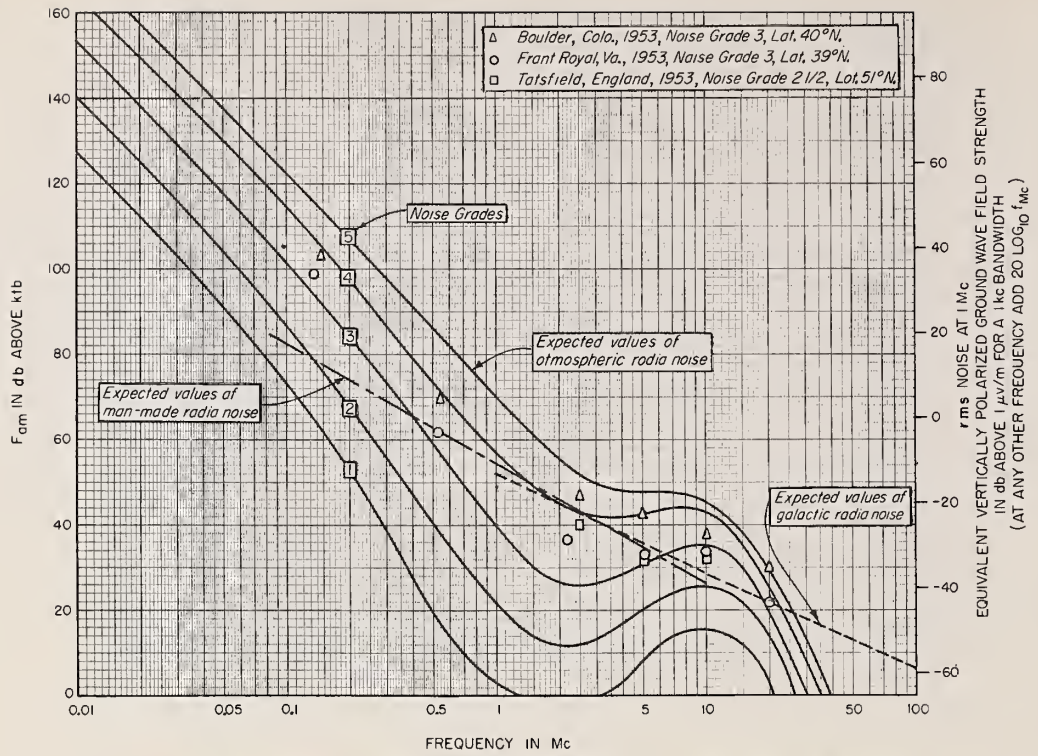
FIGURE 22. *Median values of radio noise expected for a short vertical antenna.*
For the time block, 0800–1200, summer.
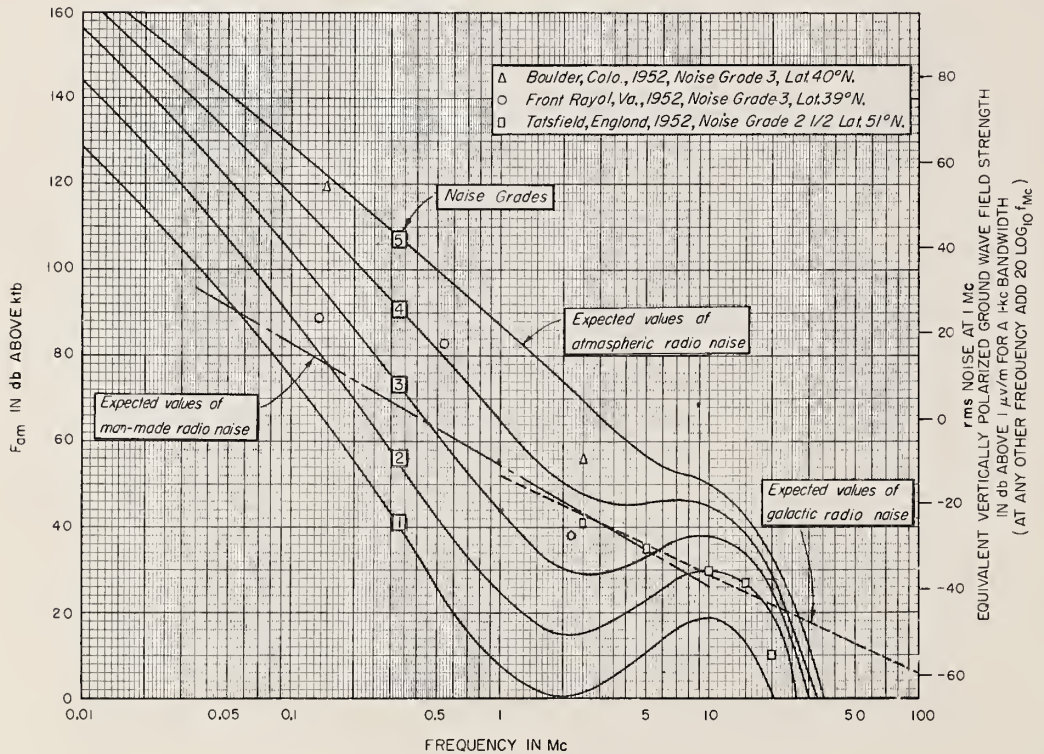
FIGURE 23. *Median values of radio noise expected for a short vertical antenna.*
For the time block, 1200–1600, summer.
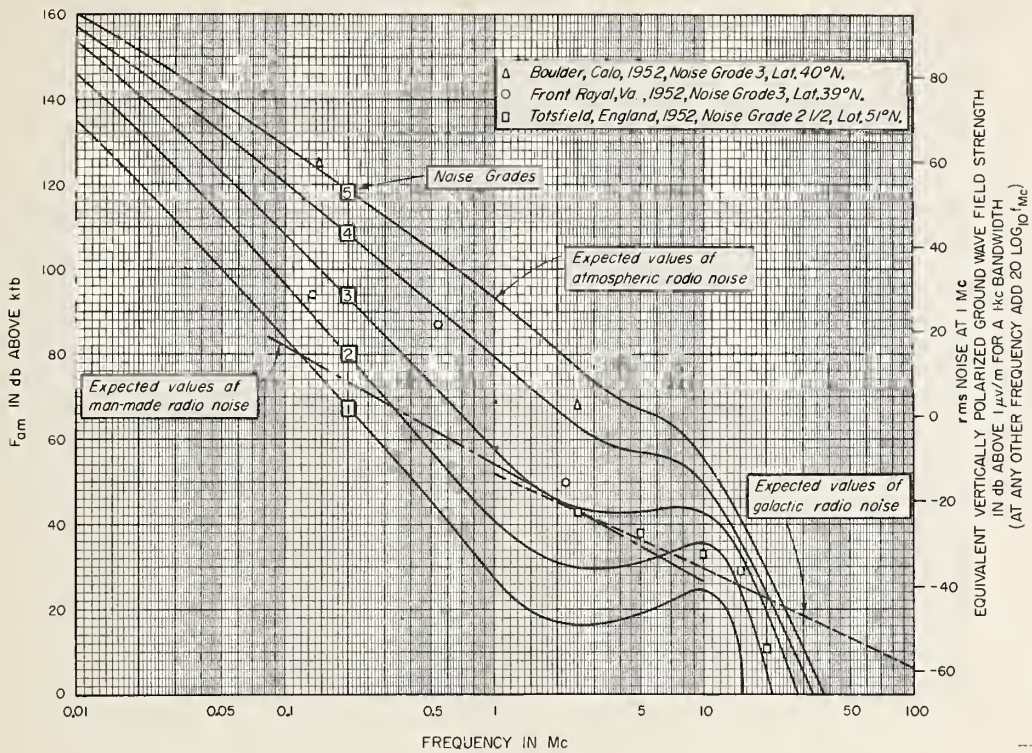
FIGURE 24. *Median values of radio noise expected for a short vertical antenna.*

For the time block, 1600–2000, summer.
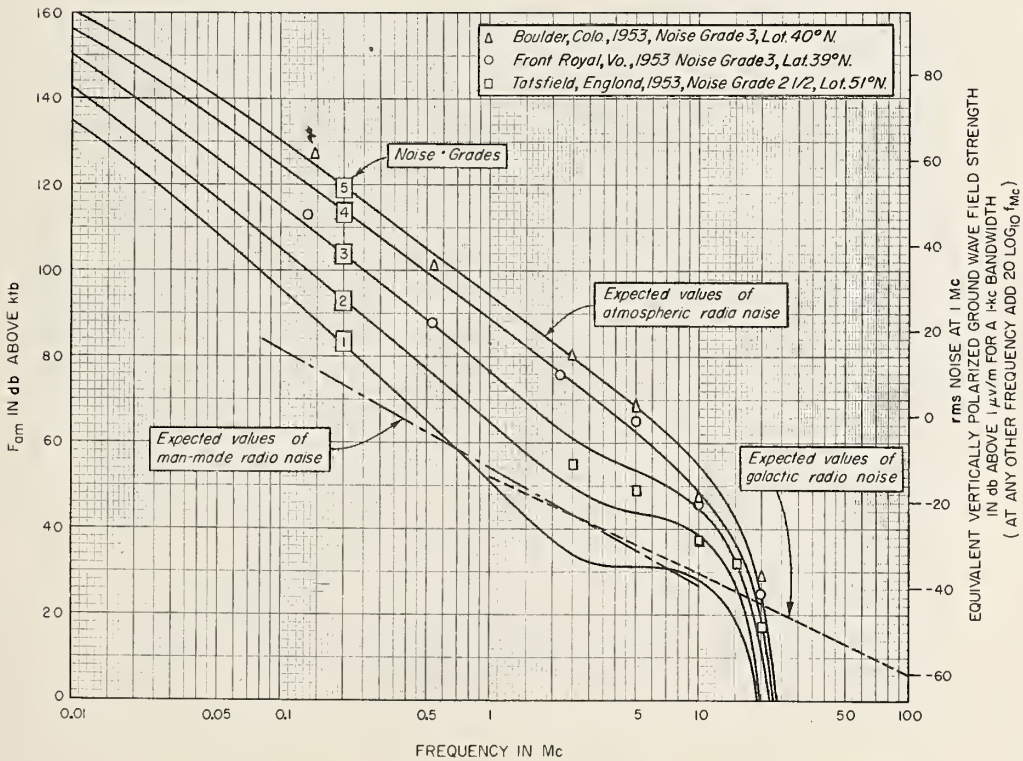
FIGURE 25. *Median values of radio noise expected for a short vertical antenna.*

For the time block, 2000–2400, summer.

25
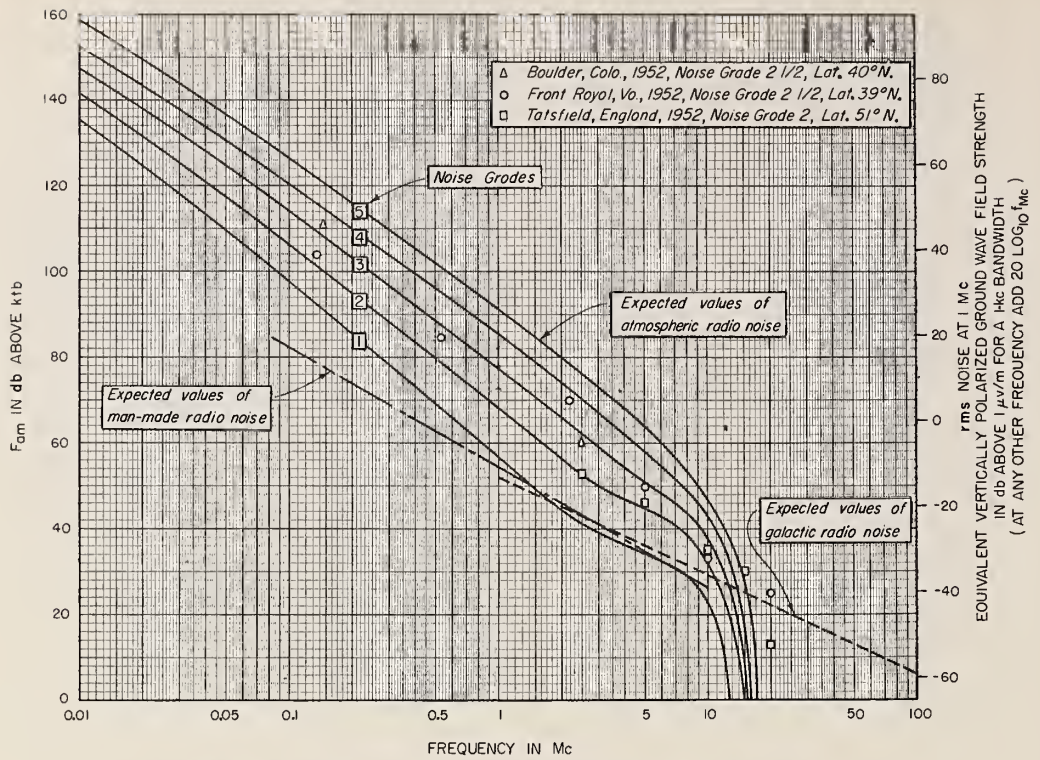
FIGURE 26. *Median values of radio noise expected for a short vertical antenna.*
For the time block, 0000–0400, fall.
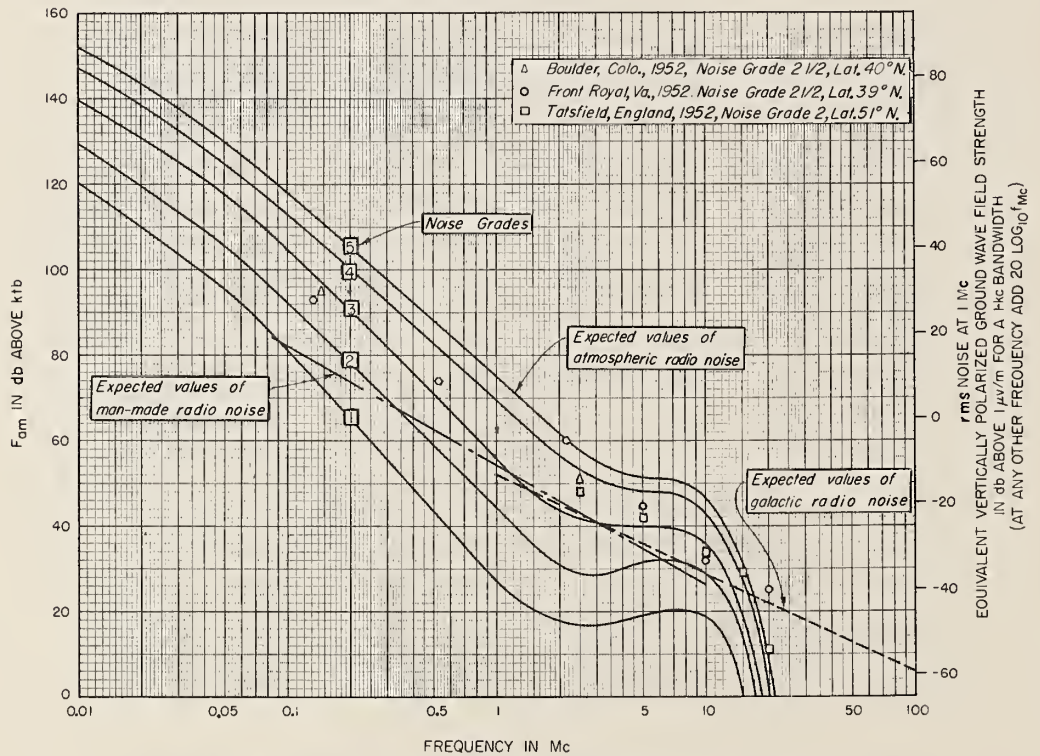
FIGURE 27. *Median values of radio noise expected for a short vertical antenna.*
For the time block, 0400–0800, fall.

26
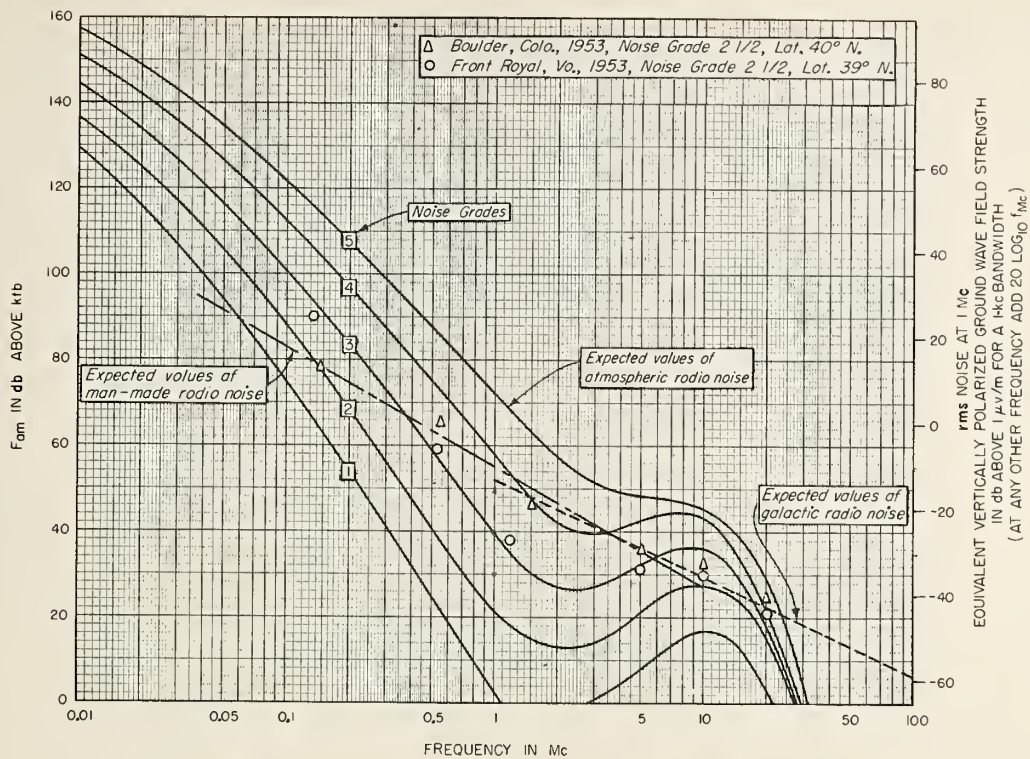
FIGURE 28. *Median values of radio noise expected for a short vertical antenna.*
For the time block, 0800–1200, fall.
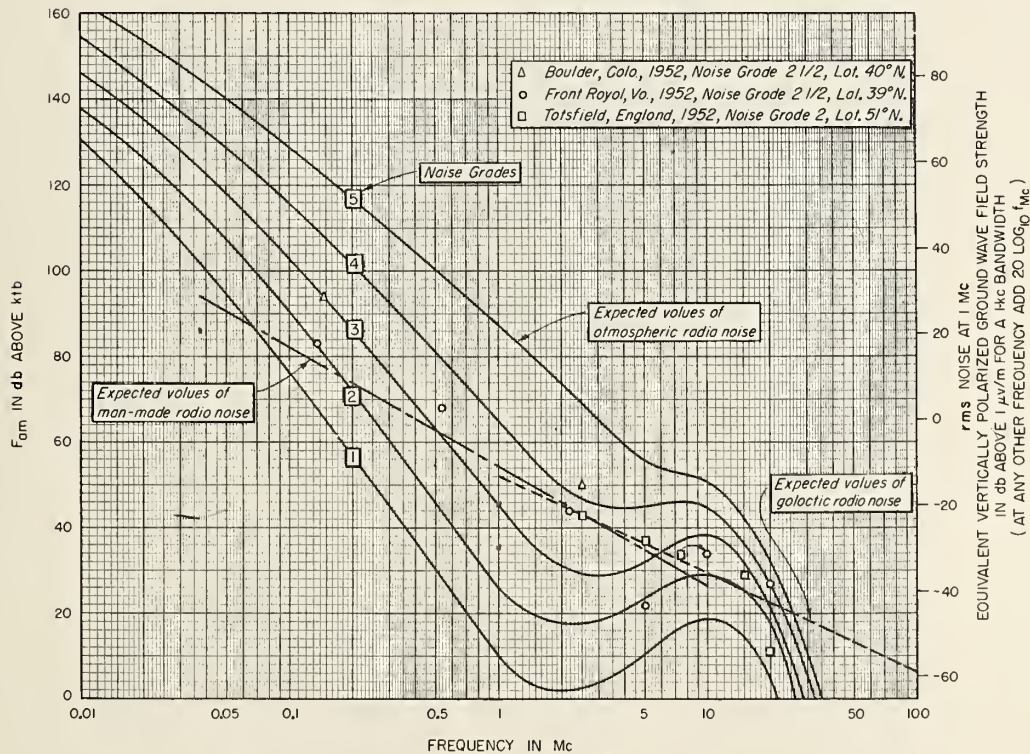
FIGURE 29. *Median values of radio noise expected for a short vertical antenna.*
For the time block, 1200–1600, fall.

27
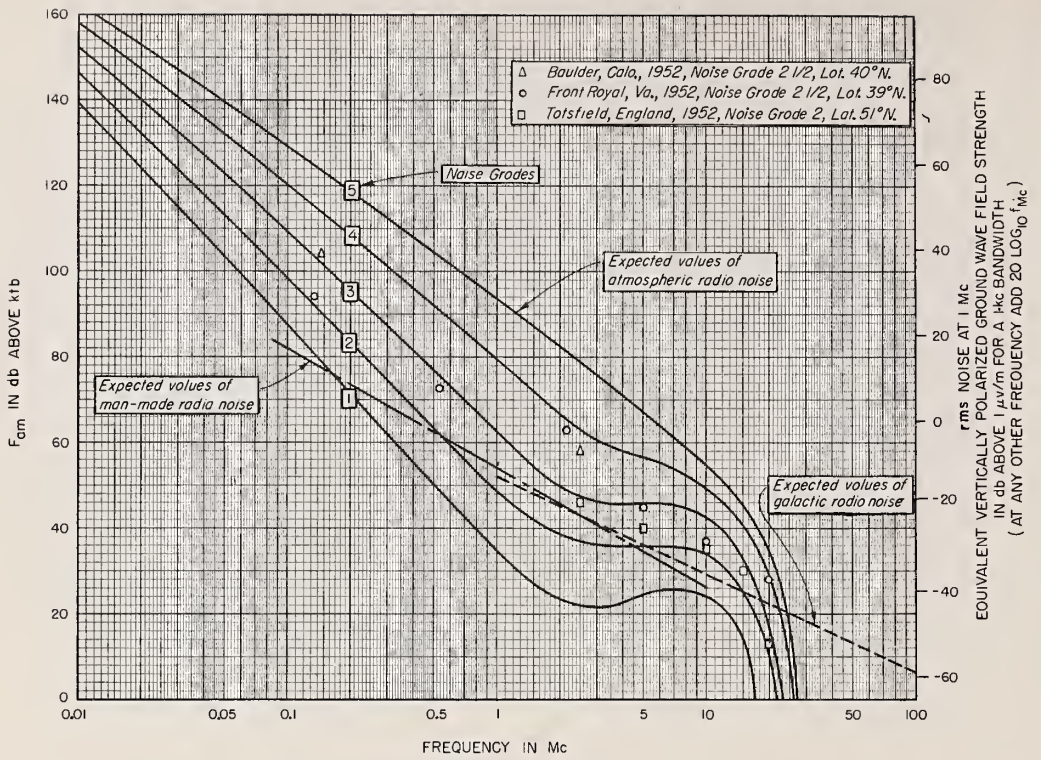
FIGURE 30.   *Median values of radio noise expected for a short vertical antenna.*
For the time block, 1600–2000, fall.
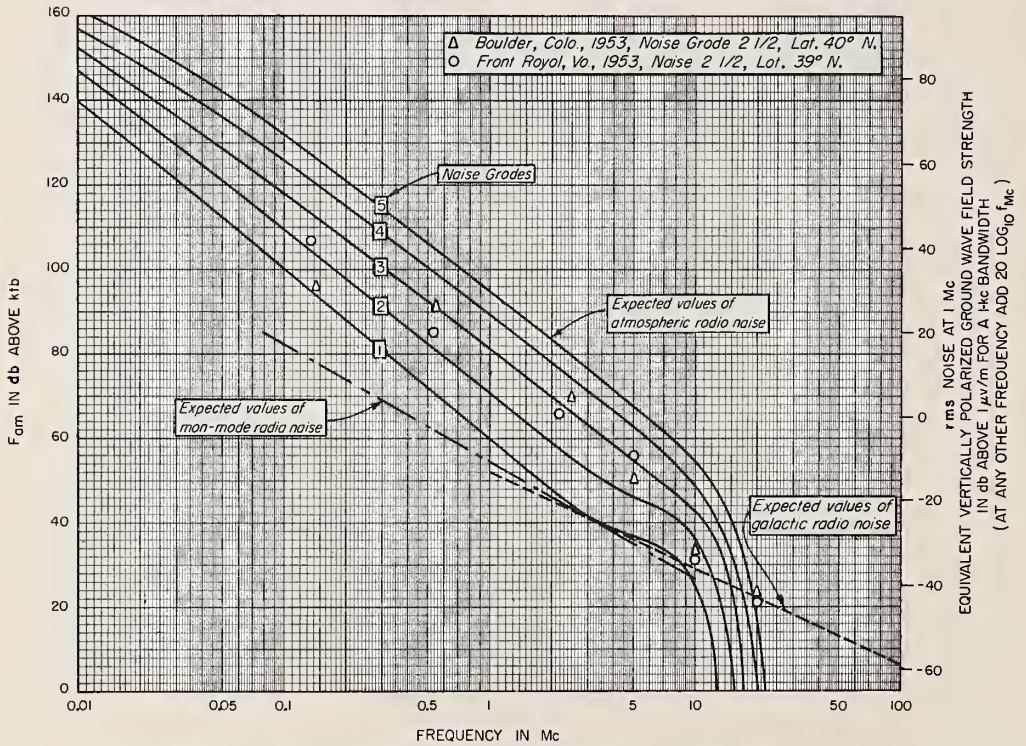
FIGURE 31.   *Median values of radio noise expected for a short vertical antenna.*
For the time block, 2000–2400, fall.
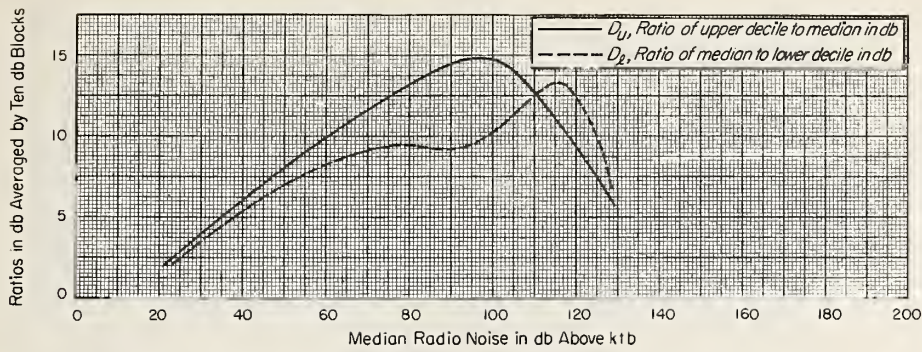
FIGURE 32. *Variations from the median radio noise levels.*

Ratios of upper deciles to medians and medians to lower deciles of radio noise levels averaged by 10-db intervals as a function of median radio noise level.
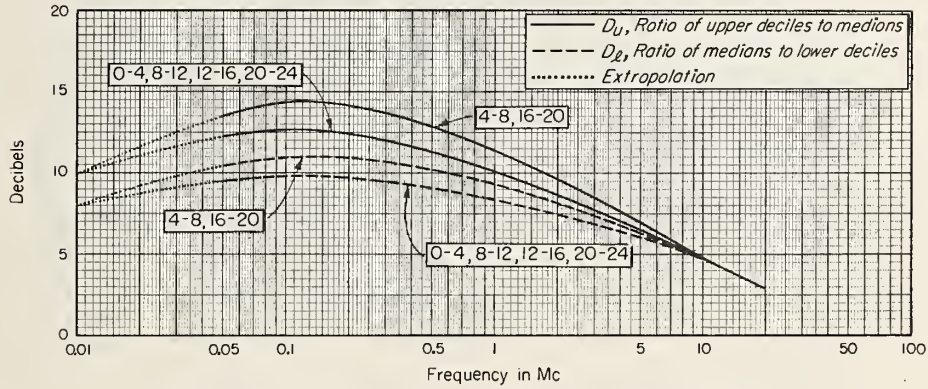
FIGURE 33. *Variations from the median radio noise levels.*

Average ratios of upper deciles to medians and medians to lower deciles of radio noise levels as a function of frequency for 4-hour time blocks.

29
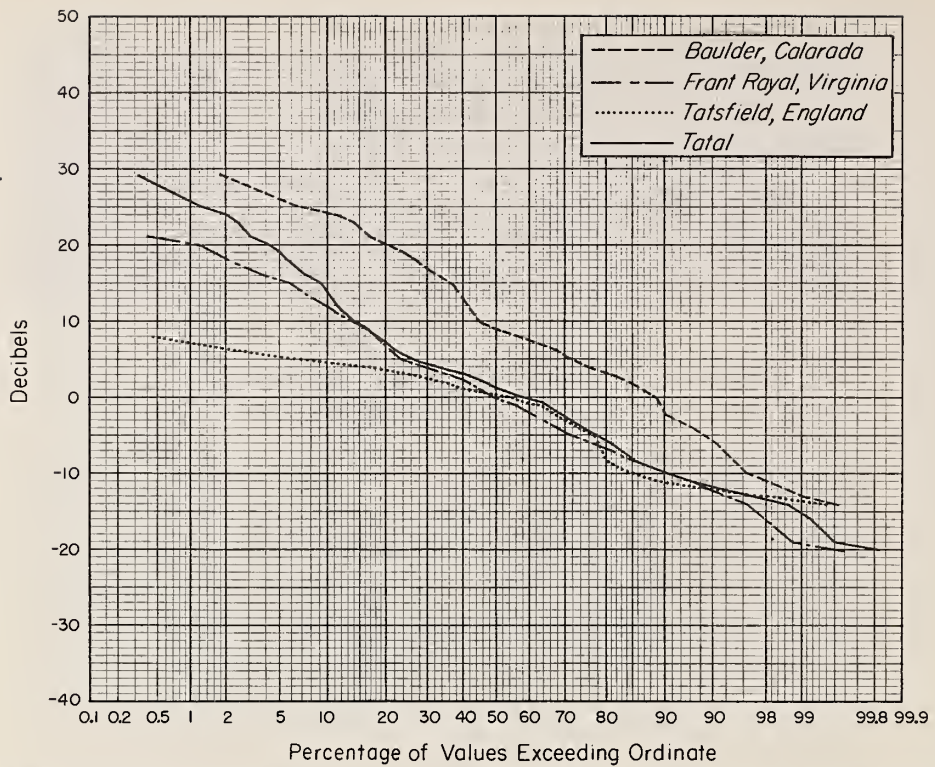
FIGURE 34. *Distribution of the deviations of the measured time-block medians from the prediction curves.*
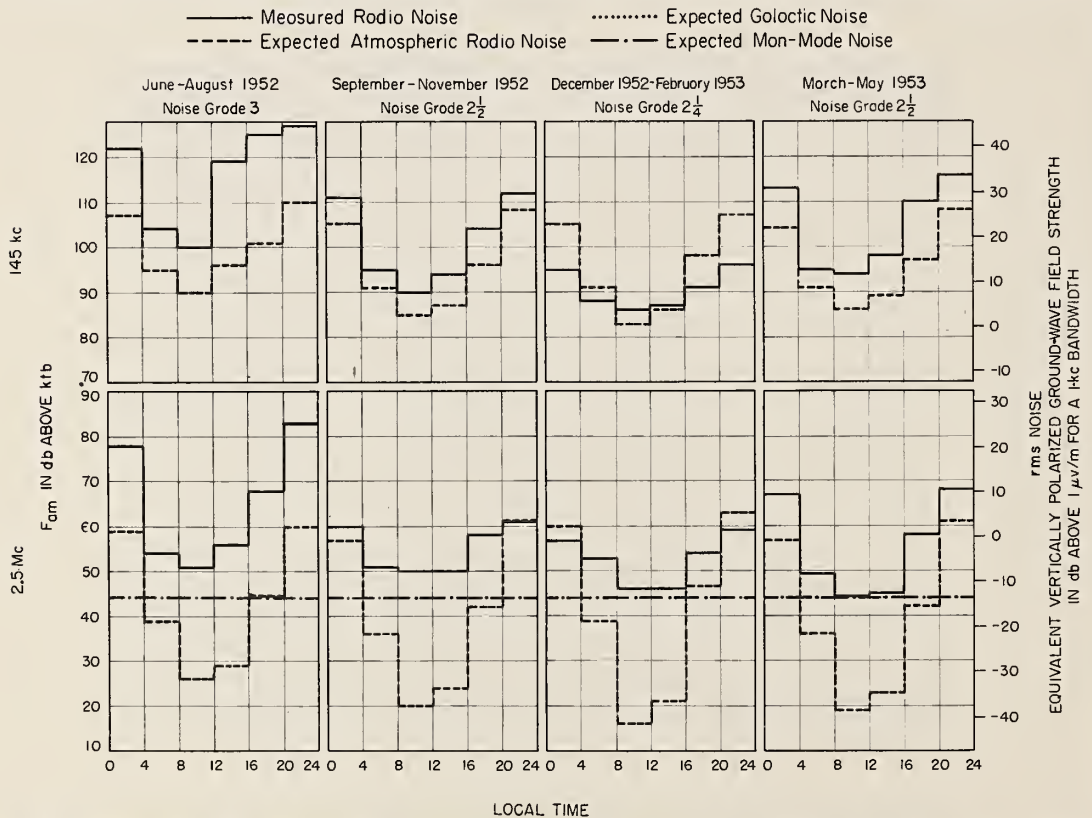
FIGURE 35. *Median radio noise levels during 4-hour time blocks for a short vertical antenna at Boulder, Colo., latitude 40° N.*
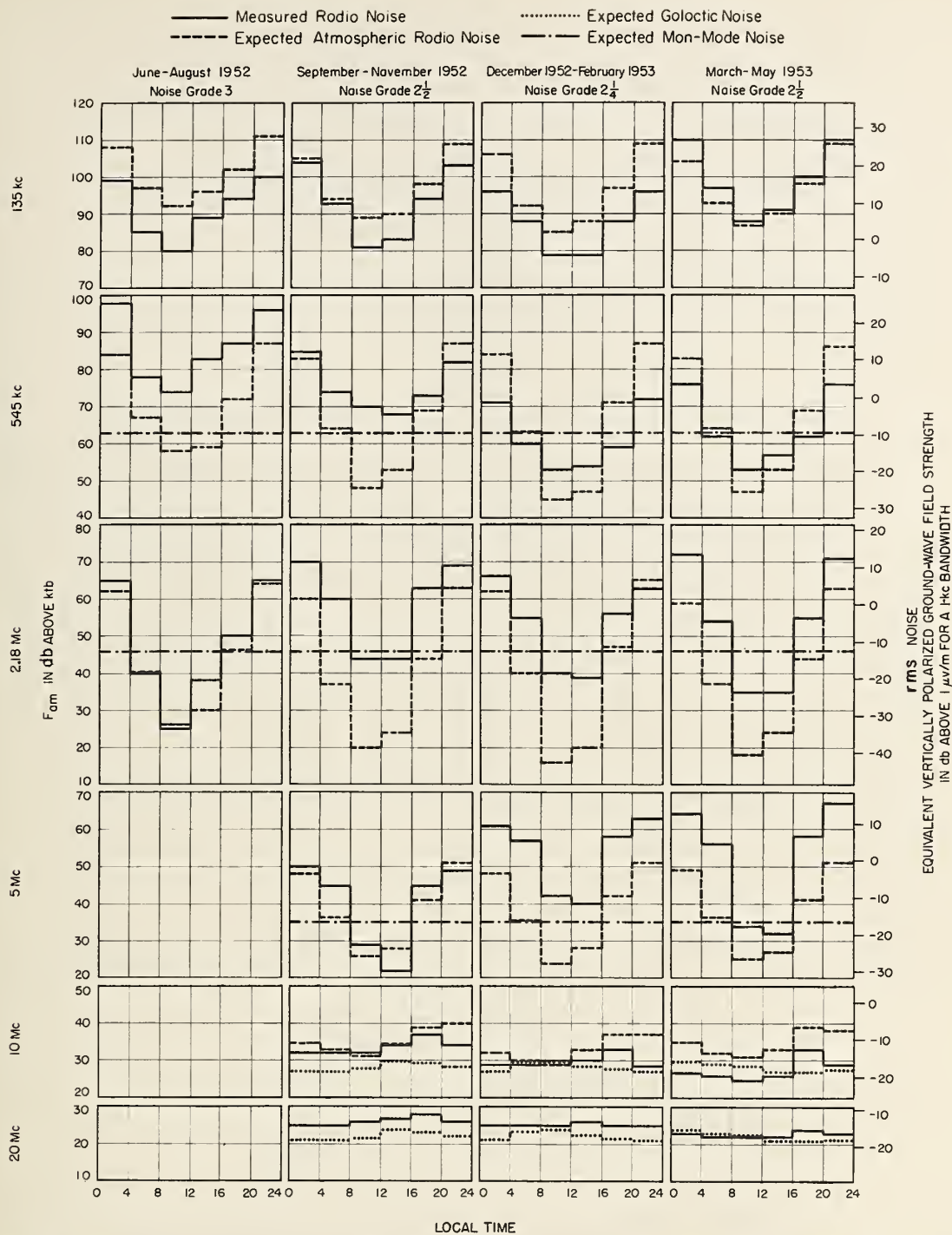
FIGURE 36.   *Median radio noise levels during 4-hour time blocks for a short vertical antenna at Front Royal, Va., latitude 39° N.*

31
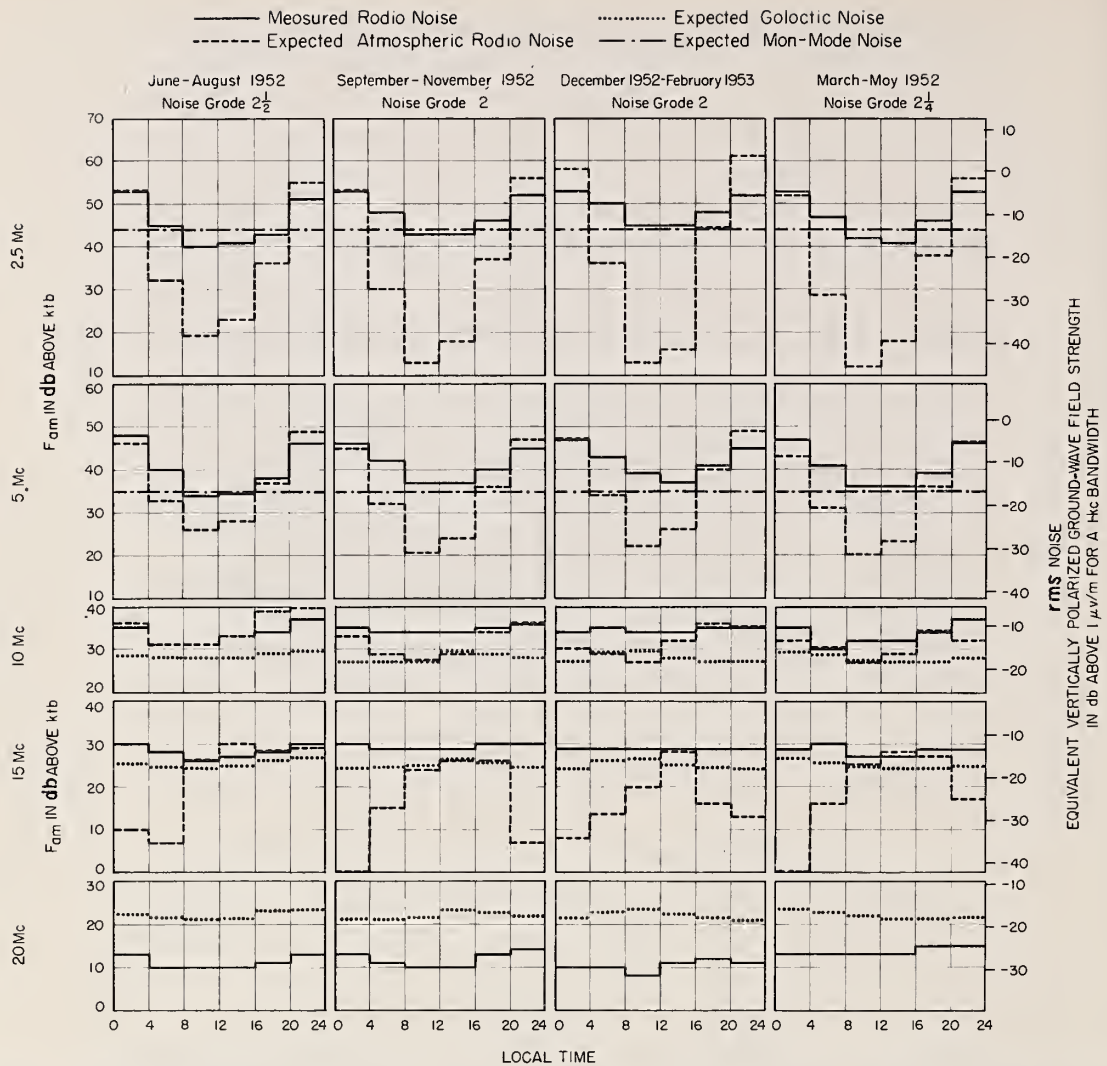
FIGURE 37.   *Median radio noise levels during 4-hour time blocks for a short vertical antenna at Tatsfield, England, latitude 51° N.*
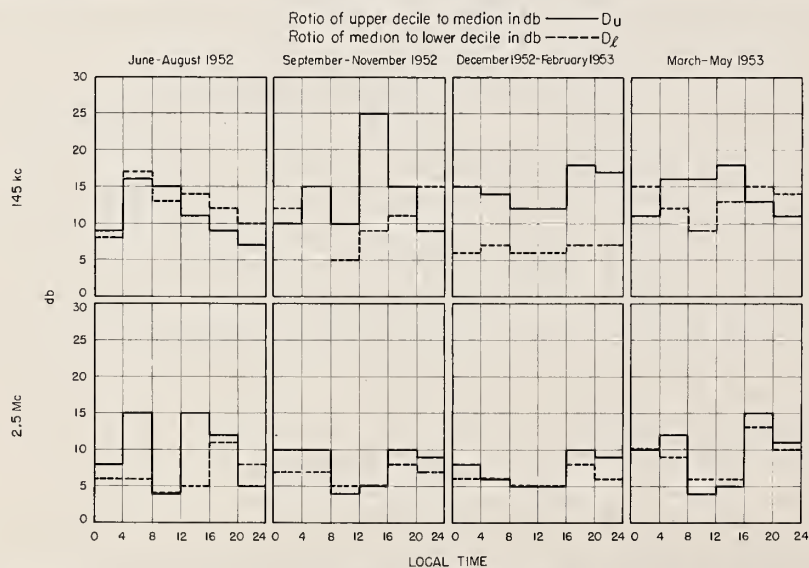

FIGURE 38.   *Deviations from the median radio noise levels measured during 4-hour time blocks for a short vertical antenna at Boulder, Colo.*

Ratio of upper decile to median in db ———— D_u
Ratio of median to lower decile in db ‐‐‐‐‐ D_ℓ
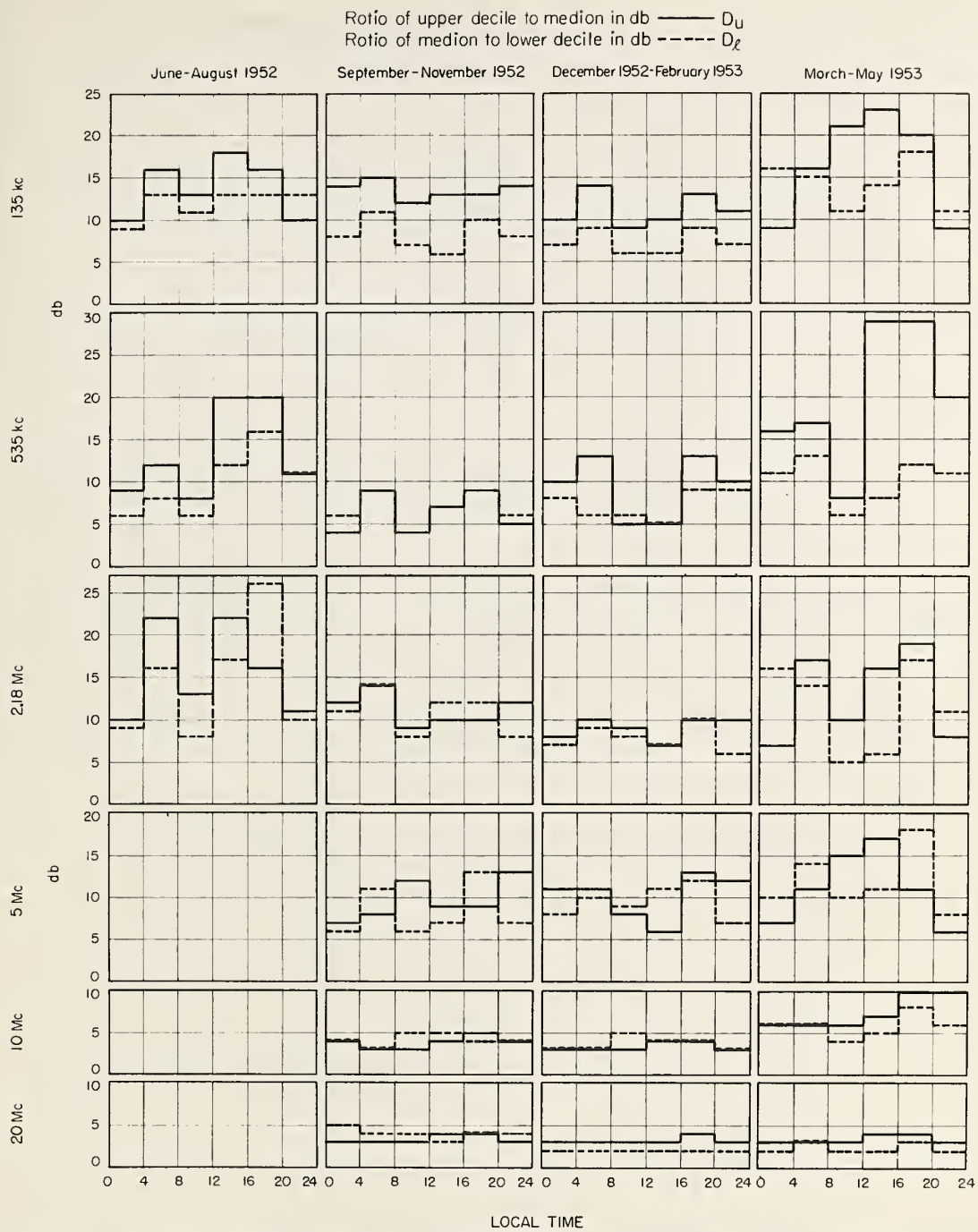
FIGURE 39. Deviations from the median radio noise levels measured during 4-hour time blocks for a short vertical antenna at Front Royal, Va.

33
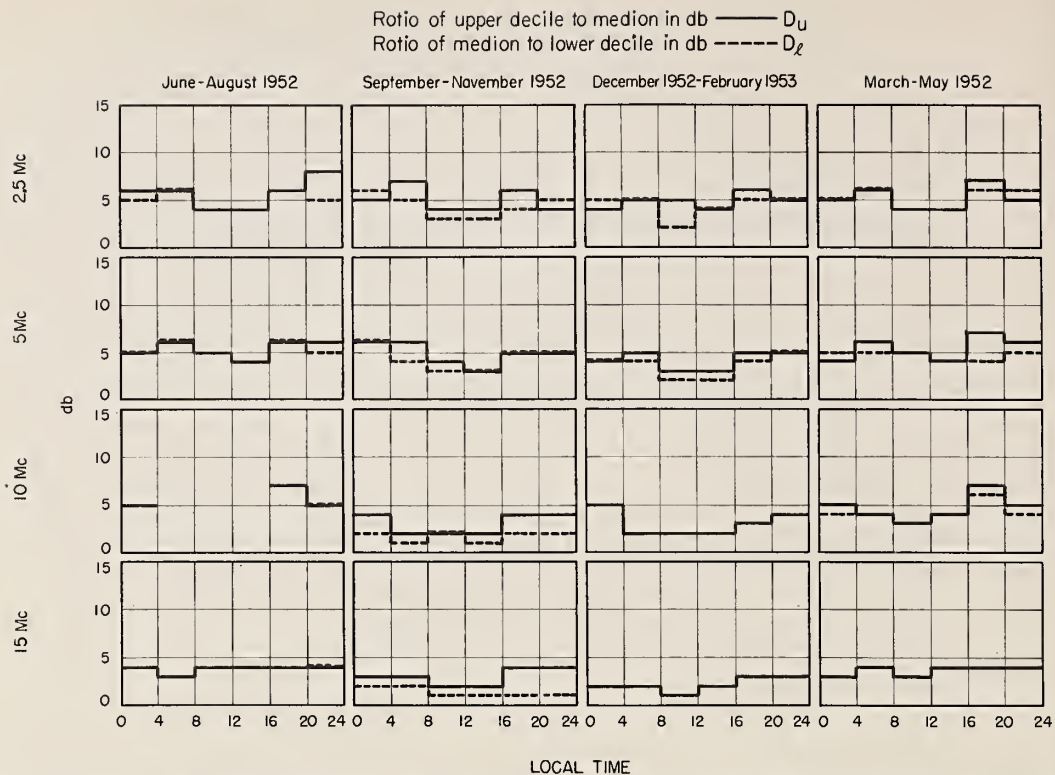
FIGURE 40. *Deviations from the median radio noise levels measured during 4-hour time blocks for a short vertical antenna at Tatsfield, England.*
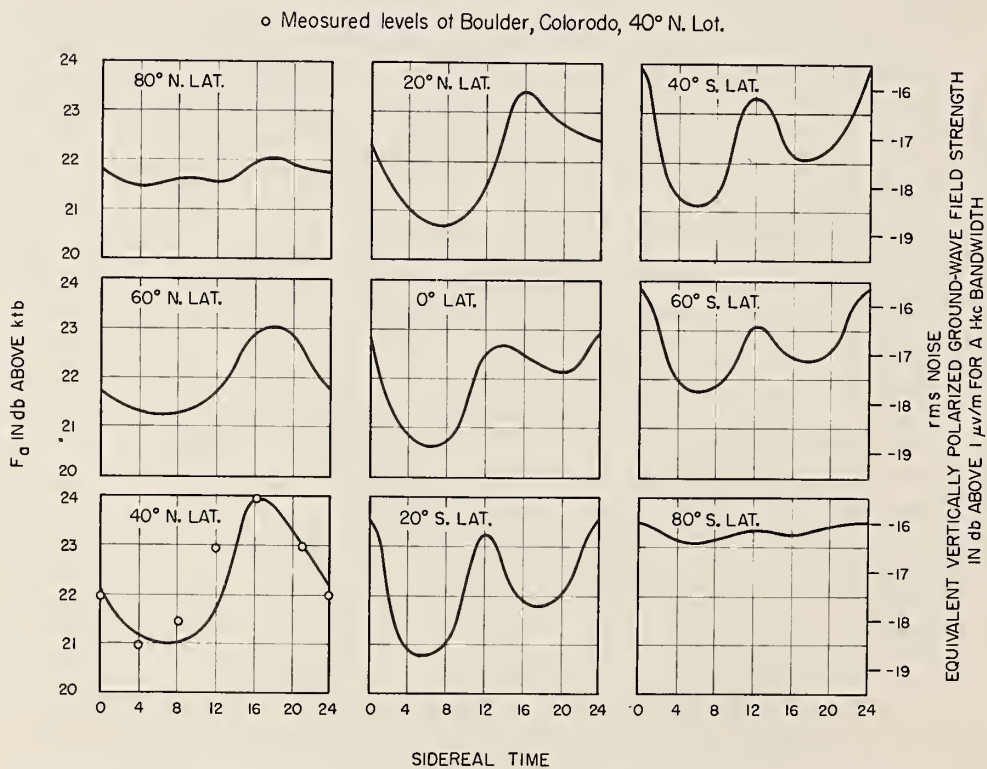

FIGURE 41. *Galactic radio noise levels expected for a half-wave vertical antenna at 20 Mc.*
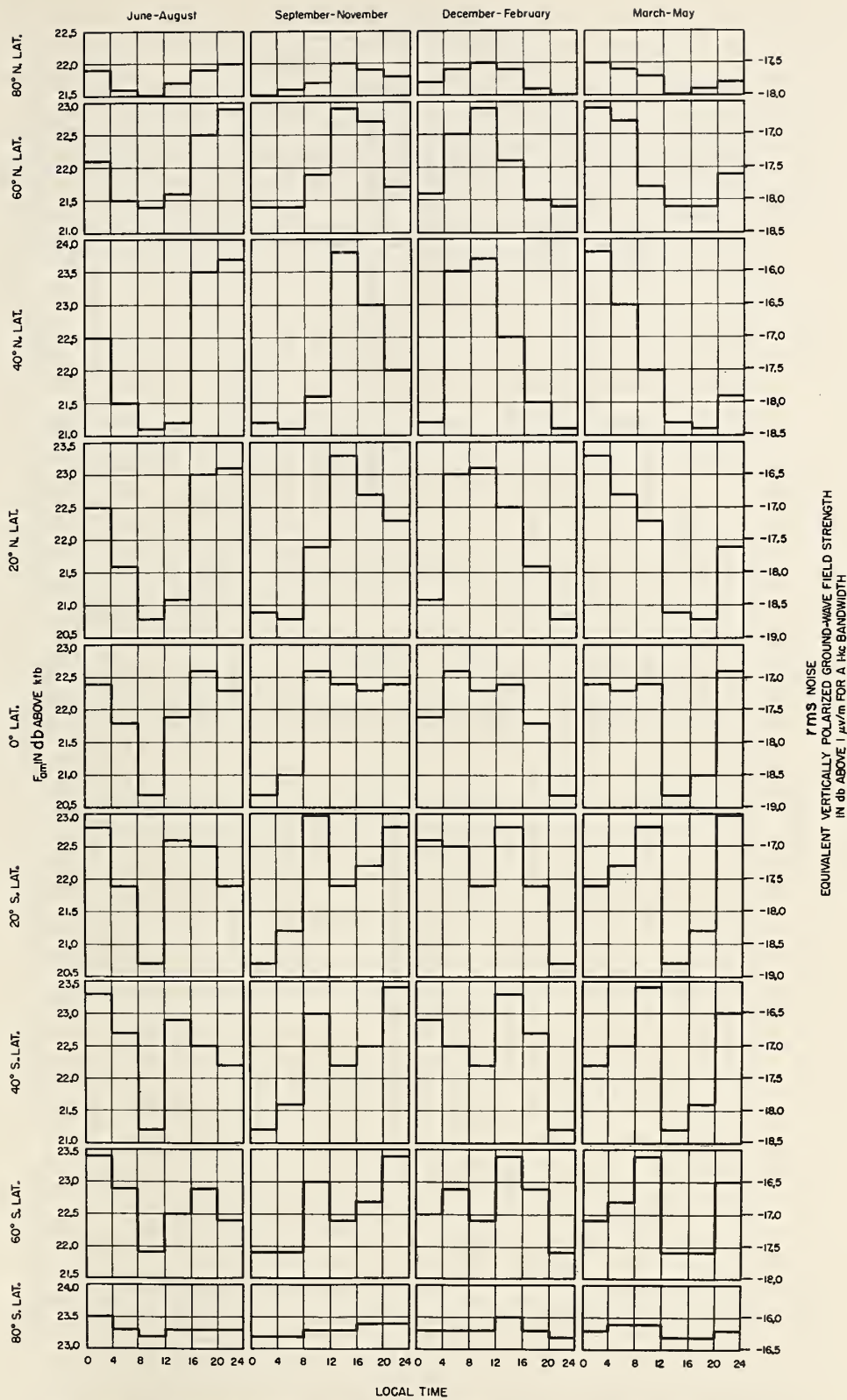
FIGURE 42. *Median galactic radio noise levels expected during 4-hour time blocks for a half-wave vertical antenna at 20 Mc.*

35
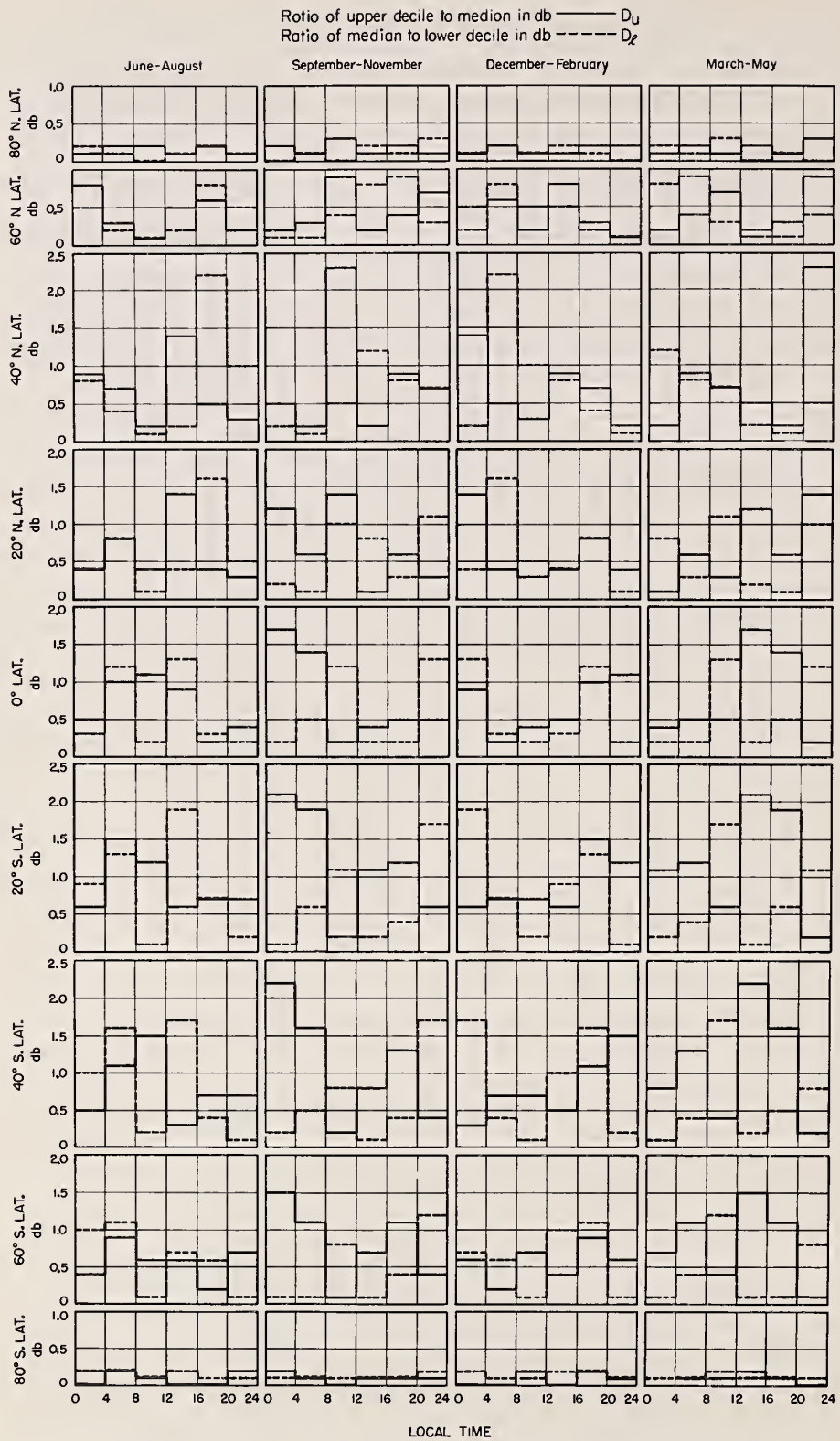
FIGURE 43. *Deviations from the median galactic radio noise levels during 4-hour time blocks for a half-wave vertical antenna.*

BOULDER, COLO., June 28, 1954.

36